Accepted Manuscript

Significance of the early Jurassic Garamilla formation in the Western Nordpatagonian Massif

Leonardo Benedini, Daniel Gregori

PII: S0895-9811(13)00053-9

DOI: 10.1016/j.jsames.2013.03.016

Reference: SAMES 1170

To appear in: *Journal of South American Earth Sciences*

Received Date: 26 October 2012

Accepted Date: 21 March 2013

Please cite this article as: Benedini, L., Gregori, D., Significance of the early Jurassic Garamilla formation in the Western Nordpatagonian Massif, *Journal of South American Earth Sciences* (2013), doi: 10.1016/j.jsames.2013.03.016.

Graphical Abstract (for review)

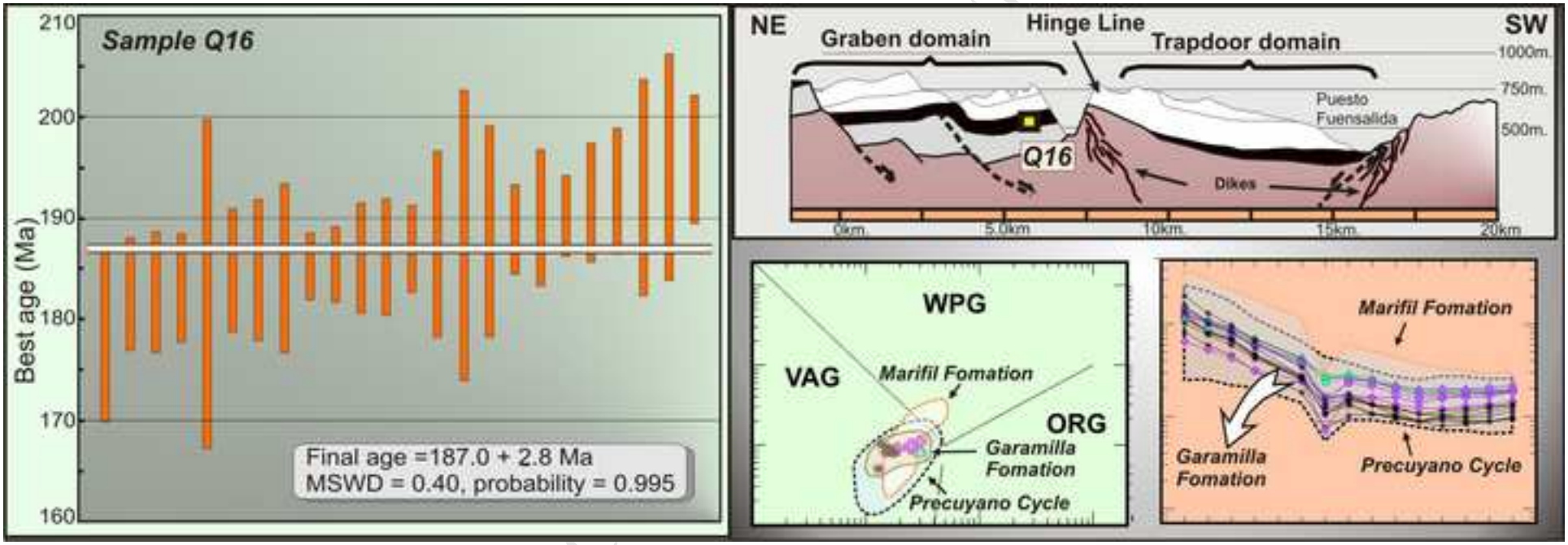

Research highlights

- We study the volcanites of Garamilla Formation in western Nordpatagonian Massif.
- It is composed by three units with andesitic, dacitic and rhyolitic compositions.
- Radiometric dating indicates Early Jurassic time for development of the volcanic system.
- Field evidences show a half graben and trapdoor structure related to eruption.
- It is comparable with equivalent units in the Neuquén Basin and Nordpatagonian Massif.

SIGNIFICANCE OF THE EARLY JURASSIC GARAMILLA FORMATION IN THE WESTERN NORDPATAGONIAN MASSIF

Leonardo Benedini* and Daniel Gregori

INGEOSUR, Cátedra de Geología Argentina, Departamento de Geología, Universidad Nacional del Sur, San Juan 670, 8000 Bahía Blanca, Argentina.

lbenedini@criba.edu.ar,usgregor@criba.edu.ar

*Corresponding author: tel: +54-291-4595101 ext: 3031. lbenedini@criba.edu.ar

Abstract

By means of facial, stratigraphic, petrographic, geochemical and geochronological studies we characterize the Garamilla Formation, cropping out in the western Nordpatagonian Massif.

The studies of these volcanic rocks reveal an Early Jurassic volcanic episode formed by three volcanic units that change from normal calc-alkaline to high-K calc-alkaline series. Other geochemical features reveal a progressive change from an initial subduction-related volcanism to one intraplate-related volcanism. This volcanic episode is temporally and geochemically equivalent to those volcanic units located in half-grabens in several areas of the Neuquén Basin. The volcanic units were erupted into different structural designs. A portion of its depocenter was interpreted as a transtensional half-graben, whereas the other exhibits a trapdoor structure. The lineament trends that bound the volcanic system were also recognized in western Nordpatagonian Massif, and were assigned to the Gondwanide Orogeny.

Key words: Volcanism, Early Jurassic, Garamilla Formation, Western Nordpatagonian Massif, Argentina.

1. Introduction

The Early Mesozoic tectonic history of the southern South America region is closely linked to the rupture and separation of the Gondwana Supercontinent, which began in the Triassic with the formation of intracontinental rifts. Later, in the Lower Jurassic, the western margin of South America was affected by the development of subduction systems. As a result, oblique batholiths (Pankhurst et al., 1992; Rapela and Pankhurst, 1992;Rapela et al., 2005) appear in the western margin of Patagonia, due to convergent conditions during the Early Jurassic. Therefore, the major crustal extension in the Andean margin was related to a trench roll-back, which would be responsible for the associated subduction extension that characterizes most of this period (Mpodozis and Ramos, 2008).

The extra-Andean Mesozoic volcanism in Patagonia is related to large-scale half-grabens, mainly oriented NNW–SSE as suggested by Gust et al. (1985), Homovc et al. (1996) and Feraud et al. (1999).

Specifically, the western Nordpatagonian Massif was subject to major extensional stress, related to the break-up of Gondwana during Triassic times, with the development of continental rifts.

During the Early Jurassic, ENE–WSW oriented extensional conditions prevailed in this area, promoting the development of extensive volcanism and the opening of the marine Neuquén Basin located immediately west of the Nordpatagonian Massif. In the eastern Nordpatagonian Massif, the Jurassic volcanic pile is composed of extensive ignimbrite deposits of the Marifil Complex, which are chemically, petrologically and isotopically uniform. The overall activity persisted over some 20 Ma. Pankhurst and Rapela (1995) suggest that rifting and break-

up of the Gondwana supercontinent produced extensive melting of the lower crustal, necessary for the development of this huge magmatism.

In the western Nordpatagonian Massif, the Jurassic units outcrop between Piedra del Aguila, Comallo, and the La Esperanza localities, and are represented by volcanic and subvolcanic rocks. Due to the absence of detailed mapping, profiling, radiometric dating, and geochemical data, these rocks were compared with apparently similar volcanic sequence outcrops more than 200 km south. Therefore they were assigned to the Garamilla Formation by Cucchi et al. (1998).

For the first time, this paper documents facies characteristics, stratigraphy and the geochemistry of the volcanic and subvolcanic sequences erupted in a key area represented by the boundary between the western Nordpatagonian Massif and the Neuquén Basin. The study focuses on analysis of the volcanic rocks outcropping in the area east of the Limay River between 69°47´–70° 00´ W and 40° 04´–40° 10´ S. This paper also reports geochronological studies, which allow comparison with coeval sequences recognized in the Neuquén Basin and the eastern Nordpatagonian Massif. In addition, we aim to better understand the geochemical and petrologic evolution of the volcanism, its tectonic setting and the interrelationship between volcanism and the regional lineaments. Ultimately, we attempt to correlate equivalent volcanic events of the central area of the Neuquén Basin and central Nordpatagonian Massif.

2. Local geology

The study area is located in the western sector of the Nordpatagonian Massif that mostly occupies northern Patagonia (Fig.1) where three tectonomagmatic

cycles can be recognized. The older one belongs to the Pampean Orogeny (Vendian-Middle Cambrian) and is represented by low-degree micaceous schists, quartzites and phyllites of the Cushamen Formation (Volkheimer, 1964). However, new dating of detrital zircons in equivalent rocks outcropping in the area of Río Chico by Hervé et al. (2008) demonstrated a Carboniferous age for this metasedimentary sequence.

The low-degree metamorphic rocks were intruded by tonalite, granodiorite and granite of the Mamil Choique Formation (Volkheimer, 1964; Sesana, 1968; Ravazolli and Sesana, 1977; Nullo, 1979; Núñez and Cucchi, 1990 and 1997). This unit represents the Famatinian Orogeny and forms near all the pre-Triassic outcrops in the Limay River area in the western Nordpatagonian Massif. Radiometric dating, using Rb-Sr isochrones (Linares et al., 1988; Cingolani et al., 1991; Dalla Salda et al., 1994), indicates a Silurian-Devonian age for the type of area. Later studies by López de Luchi et al. (1999, 2000), Cerredo et al.(2000) and Pankhurst et al. (2006) show that this magmatic event can be related to the Gondwana Orogeny. Neither the Pampean nor the Famatinian rocks are displayed in Figure 1 in order to avoid confusion.

Covering in non-concordance the above described units appears the Triassic Los Menucos Formation, which represents a continental rift. Above all the described units appears a set of rhyolitic and dacitic ignimbrites, rhyolitic lava-flows, and tuffs, which were assigned by Nullo (1978) to the Garamilla Formation, and originally correlated with the Los Menucos Formation.

This unit outcrops mainly in the area between the Limay River, La Esperanza and Laguna Blanca and has been regionally studied by Volkheimer (1964), Coira (1979), Núñez and Cucchi (1990, 1997), and Benedini and Gregori

(2012). A reliable age (188 ± 1.5 Ma, U-Pb in zircon) for this unit was obtained by Franzese et al. (2002) in rock outcrops more than 200 km south of the studied area, near the type locality. That age, in conjunction with the lithological characteristics of the Garamilla Formation, allows correlation with the Marifil Formation in the eastern portion of the Nordpatagonian Massif (Fig.1).

In the eastern border of the Neuquén Basin, near the Limay River, appear the Piedra del Aguila and Sañicó Formations (Precuyano deposits), composed of a sedimentary sequence of alluvial and fluvial environments and andesitic and rhyolitic lava-flows and volcaniclastic deposits. The first unit was dated by Spalletti et al. (2010) using U-Pb in zircons obtaining an age of 191.7 ± 2.8 Ma. Jurassic basic volcanic rocks assigned to the Taquetrén Formation outcrop in the southwestern border of the Nordpatagonian Massif. Jurassic magmatic arc-related igneous rocks appear in the Andean domain of northern Patagonia and were assigned to the Subcordilleran Batholith. The Tertiary and Quaternary are represented by tuffaceous material and unconsolidated sedimentary deposits.

3. Volcanic stratigraphy of the Garamilla Formation

The detailed profiling of the studied area allows us to differentiate three volcanic units and a set of rhyolitic dikes. A descriptive scheme of effusive and pyroclastic rocks is adopted during the facies descriptions (McPhie et al., 1993; Branney and Kokelaar, 2002)

The first volcanic unit comprises lava-like ignimbrites, porphyritic massive rhyolite and microgranular massive rhyolite. The second is composed of porphyritic massive andesite and dacite, lapilli-tuffs and eutaxitic lapilli-tuffs of dacitic composition. The third unit includes tuffs, lapilli-tuffs, massive tuff-

breccias, massive lithic breccias and porphyritic massive and flow-banded rhyolite (Fig. 2).

3.1. First volcanic unit

This unit is widely represented in the area located between Cañadón Mencué and Cañadón Quili Mahuida by a) lava-like ignimbrites, b) porphyritic massive rhyolite and c) microgranular massive rhyolite.

a) Lava-like ignimbrites (lava-like T)

The lava-like ignimbrites outcrop 1 km north of the Puesto Quiñenao ending in the Cañadón Quili Mahuida. They extend more than 5 km in an ENE–WSW direction, displaying a remarkable homogeneity along the overall path, and covering an area of 10 km^2 (Fig. 2). The sequences are uniform stratified with individual flows ranging from 0.20 to 1 m thick. Columnar jointing is usually recognized (Fig. 3A). Microscopically, they show “granophyric texture”, (McArthur et al., 1998) composed of a mosaic of equigranular anhedral to subhedral crystals of quartz and K-feldspar (Fig. 3B) with less content of biotite. Individual crystals are less than 200μ. Lithic fragments of granitic rocks are sparse and range from 1 to 4cm in size.

b) Porphyritic massive rhyolite (pmR)

The massive rhyolitic lava-flows appear northwest of Puesto Martinez, between Cañadón Mencué and Cañadón Quili Mahuida (Figs. 2 and 3C). The relationship with the above described facies is complex and most of the time seems to be interbedded. However, when their morphological features have not

been preserved, the difference between both facies is difficult to recognize. They are pale pink to orange, less than 100 m thick and characterized by porphyritic textures defined by euhedral to subhedral K-feldspar, plagioclase and quartz phenocrysts arranged in a fluidal groundmass composed of microcrystalline quartz. The crystals have a moderate sericitic alteration, while biotite and plagioclase are altered to chlorite and calcite (Fig. 3D). Porphyritic textures, with high temperatures of devitrification in the groundmass, that could be internally massive or flow foliated (Mc Phie et al. 1993), define coherent lithofacies in lavas as synvolcanic intrusions.

c) Microgranular massive rhyolite (mmR)

The microgranular massive rhyolite has an oval shape, 2 km in diameter, rounded in morphology and internally massive and coherent (Figs. 2 and 3E). It is pale pink to orange in color and its texture is microcrystalline to porphyritic. The microcrystalline texture represents up to 70% of the sample and is formed by euhedral to subhedral quartz and K-feldspar with micrographic textures. Micrographic textures (Fig. 3F) evidence eutectic crystallization conditions. Plagioclase crystals are frequently altered to calcite and sericite. Biotite is euhedral and shows an incipient oxidation and chloritization. Autoclastic facies were not recognized.

3.2. Second volcanic unit

This unit is represented in the Cañadón Mencué and near Puesto Fuensalida and is composed of a) porphyritic massive andesite and dacite, and b) massive lapilli-tuffs and eutaxitic lapilli-tuffs of dacitic composition (Fig. 2).

a) Porphyritic massive andesite and porphyritic massive dacite (pmA and pmD)

These lithofacies are exposed in the vicinity of Cañadón Mencué and near the Limay River, where they are covered by a succession of massive lapilli-tuffs and porphyritic massive rhyolite belonging to the third eruptive event (Fig. 4A). The best outcrops are located near Puesto Fuensalida, where they cover, unconformably, the Gondwana granites, without record of the first eruptive unit. Small outcrops were also detected west of Puesto Quiñenao resting on the lava-like ignimbrites of the first volcanic unit. The thickness reaches 60 m near Puesto Fuensalida. These facies exhibit a porphyritic texture consisting of euhedral to subhedral crystals of plagioclase, 1.5 mm long, together with amphibole phenocrysts embedded in a trachytic groundmass. Dacitic lava-flows have lower proportions of mafic minerals and are composed of K-feldspar, plagioclase, quartz and biotite. The groundmass shows a pilotaxitic texture with a strong orientation of plagioclase microphenocrysts. The plagioclase is altered to epidote (Fig. 4B).

b) Massive lapilli-tuffs (mLT)

The gray-blue to pale-violet massive lapilli-tuffs consist of deformed vesicular juvenile fragments and fragmented crystals disposed in a fine-grained matrix. A few kilometers west of Puesto Quiñenao, the massive lapilli-tuffs display eutaxitic texture (emLT) partially devitrified (Fig. 4C). The subhedral to anhedral crystals of plagioclase are fractured and altered to epidote. Amphibole is mainly altered to epidote and iron oxides, while the biotite is altered to chlorite. The fine-grained matrix is replaced by fine-grained clay minerals (Fig. 4D).

Accessory fragments ranging from a centimeter to a millimeter are of migmatites, granites and andesitic lava-flows.

3.3 Third volcanic unit

The last unit was recognized in two localities. One includes outcrops west of Puesto Quiñenao (Fig. 4E) and the other appears between Cañadón Curru Mahuida and Cañadón Quili Mahuida and includes a) parallel bedded tuffs, b) massive lapilli-tuffs, c) massive tuff-breccias, d) massive lithic breccias and e) porphyritic massive rhyolite and flow banded rhyolite totaling about 330 m thick (Fig. 2).

a) Parallel bedded tuffs (//b T)

Pale-yellow to white tuffs consisting of finely laminated layers rich in crystals (approx. 40%) were found near Puesto Quiñenao. They usually occur towards the base of pyroclastic rhyolitic succession and commonly display a coarsening-upwards sequence together with the lapilli-tuffs (Fig. 5A). They include quartz, sanidine, plagioclase and biotite crystals. Quartz is anhedral to subhedral, usually fractured. Deformed laminas of biotite and plagioclase are altered to iron oxides and epidote respectively. The matrix corresponds to fine ash altered to sericite and clay minerals (Fig. 5B).

b) Massive lapilli-tuffs (mLT)

They are pink to white in color and contain juvenile, vesicular lithic fragments (Fig. 5C). Phenocrysts of quartz and K-feldspar are dominant, while the plagioclase and biotite are rare. The lithic fragments are generally subrounded

to subangular, 0.2 to 5 cm in diameter, and display porphyritic to spherulitic texture (Fig. 5D). The fine-grained matrix is partially silicified. This lithofacies was found near Puesto Martinez reaching 100 m thick, diminishing toward Puesto Quiñenao.

c) Massive tuff-breccias (mTBr),

These breccias cover the above mentioned facies by means of planar to slightly erosive surfaces. They are composed of lithic fragments of rhyolitic lava-flows, 10 to 20 cm in diameter, immersed in a light gray tuffaceous matrix (Fig. 5E). They present bread-crust textures indicating hot deposition and very fast cooling. Vesicular juvenile fragments were not observed. They crop out north of Cañadón Mencué (Fig. 2).

d) Massive lithic breccias (mLBr)

Massive lithic breccias were identified at the top of the pyroclastic sequence present in the northern border of the Cañadón Mencué, overlying the massive lapilli-tuffs and massive tuff-breccias. They are characterized by the presence of large amounts of lithic fragments of tuff, granite and dacite that exhibit subangular to subrounded forms. The deposit is remarkably heterogeneous and particle size ranges from a few centimeters to almost 1 m in diameter (Fig. 5F).

e) Porphyritic massive rhyolite and flow banded rhyolite (pmR and fbR)

Small, subrounded bodies with vertical flows were observed near Puesto Fuensalida and west of Puesto Quiñenao (Figs. 2 and 5G).

The lava-flows exhibit a lengthened shape and horizontal flow textures, and are

located on the top of the third volcanic unit with individual thicknesses of up to 20 m. The porphyritic texture is composed mainly of K-feldspar and quartz phenocrysts and exhibits no differences, normative or compositional,with respect to the porphyritic massive rhyolite (pmR) lithofacies of the first volcanic unit. The main difference is the flow banding of the facies here considered. The flow banding consists of nearly parallel and alternating bands with different textures, one formed by partially devitrified glass and the other by variable concentrations of spherulitic aggregates and crystals. Rounded, small spherulites of 0.5 to 1 mm size are usually fractured while those bigger than 1 cm are well preserved indicating a nearly null movement.

3.4. Dikes

Acidic dikes in the Quiñenao-Fuensalida area intrude the granitic rocks and sometimes the volcanic sequence. In the first locality (Fig. 2), they outcrop mainly near Cañadón Mencué with NW and NE strikes, dipping between 54° and 65° to the southwest and southeast. Most of the time, they are isolated, up to 100 m long and 15 m wide, with colors varying between pale-yellow and dark-orange. Sometimes dike swarm can be observed converging to a major subrounded structure that resembles a subvolcanic body emplaced in the granitic host rocks. Due to its major resistance to erosion, in comparison with granitic rocks, it forms prominent peaks in the landscape.

In the Puesto Fuensalida area, dikes are commonly 5 to 15 m wide and up to 1 km long. They are discontinuous and some portions can be covered. Microscopically, they display porphyritic and microgranular textures composed of euhedral to subhedral phenocrysts of K-feldspar (5–3 mm), quartz and

biotite. The last is altered to chlorite. The groundmass is composed of an aggregate of fine-grained quartz and K-feldspar, usually altered to sericite. Sometimes, the groundmass is glassy. The microgranular texture is characterized by the presence of spherulitic aggregates composed of quartz and K-feldspar.

4. Geochemistry of the Garamilla Formation

Fifteen samples were analyzed at ACTLABS, Canada, in order to determine the geochemical tendencies in the volcaniclastic sequence. In comparison with international geostandards, major, trace and REE elements were determined using X-ray fluorescence and inductively coupled plasma mass spectrometry.

4.1. Major elements

Geochemical analyses (Table 1) of the sequence reveal a calc-alkaline to high potassium calc-alkaline tendency (Fig. 6A) for the three volcanic units (Peccerillo and Taylor, 1976). The K_2O concentrations range from 3.5 to 4.62% in the first volcanic unit, 1.78 to 4.25% in the second and 1.88 to 3.57% in the third. The relationship K_2O/Na_2O varies between 0.94 and 1.53 in the first volcanic unit, 0.43 to 0.95 in the second and 0.36 to 1.6 in the third.

According to the abundance of K_2O and Na_2O (Fig. 6B) versus silica (Le Bas et al., 1986), samples for the first and the third volcanic units fall into the rhyolitic composition. The second volcanic unit falls into the dacitic composition.

The three volcanic units present high silica content with values that vary between 60 and 82%. However, this wide range is dominated by compositions higher than 70% of SiO_2. On the other hand, MgO values reach 2.33% in

andesitic lavas of the second volcanic unit, falling to 1.63% in the second volcanic unit. These features are revealed in highly differentiated magmas. Both the first and the third volcanic units present peraluminous characteristics, while the second is metaluminous (Fig. 6C) and shows a lower alkali concentration. Al_2O_3 contents range between 11% and 15% for the three volcanic units (Shand, 1951).

The TiO_2 concentrations also provide a measure of the geochemical evolution of the magmatic system. This oxide varies between 0.05% and 0.15% in the rhyolites (first and third volcanic units) and from 0.5% to 0.95% in dacitic to andesitic rocks, whereas the P_2O_5 varies from 0.02% to 0.05% and from 0.1% to 0.3%, respectively, for the same groups, and fractionation is linked to the crystallization of apatite. This content matches the range of average P_2O_5 of the calc-alkaline series (0.1 and 0.2%) determined by Gill (1981).

4.2. Trace elements

The composition of these rocks, according to the classifications SiO_2 versus Zr/TiO_2 (Fig. 6D) and Zr/Ti versus Nb/Y (not shown) of Winchester and Floyd (1977), confirms that they are andesites, dacites and rhyolites. The ratio Nb/Y presents a range of values generally less than 0.6 indicating that they belong to the subalkaline series. The diagram of the distribution of expanded trace elements normalized to chondrite (Thompson, 1982) in Figure 6E shows enrichment in LILE (Ba, Rb, Th, K, Sr, La, Ce) together with negative anomalies of Sr, P and Ti. The rhyolitic facies generally have more significant negative anomalies in Ti, P and Sr, and higher concentrations of LILE, indicating fractionation of apatite and titanite during magmatic evolution with enrichment in

K-feldspar. Another feature shown in Thompson's diagram (1982) is the presence of negative anomalies of Nb and Ta relative to Th and La, while the ratio Nb/Ta varies between 6.5 and 16 (Fig. 6E).

Zr concentrations range between 50 and 280 ppm and show an inverse relationship with respect to the concentrations of SiO_2. Those specimens that are more evolved show Zr concentration between 50 and 120 ppm, while the dacites and andesite vary between 150 and 280 ppm.

4.3. Rare earth elements

In the REE normalized to S1 chondrite diagram (Sun and McDonough, 1989) nearly all samples show negative Eu anomalies (Fig. 6F). Values of Eu/Eu* vary between 0.88 and 1.02. The negative Eu anomaly is associated with fractionation of plagioclase and in minor extension alkali feldspar. In all samples, enrichment of LREE and the slopes (La_N/Lu_N) are similar, indicating the cogenetic character of the series. M and HREE values indicate hornblende fractionation and the absence of garnet in the parental magma.

4.4. Tectonic discrimination

In order to establish the tectonic environment of emplacement of the studied rocks, they were plotted in diagrams Rb versus Y + Nb and Nb versus Y (Pearce et al., 1984). In both diagrams (Figs. 6G and H) acidic and intermediate samples are grouped in the fields of magmatic arc-related rocks. Relationships Ta–Yb (0.19–0.53) also show igneous environments related to convergent plate margins (volcanic arc, Pearce, 1982). Its peraluminous character could be due, in part, to the assimilation of continental crust or merging with subducted

sediment.

The LILE enrichment displayed in the diagrams of incompatible elements allows, according to Pearce (1982), suggestion that the source magma would have received contributions from fluids derived from a subducted oceanic crust. The negative anomalies of Nb and Ta corroborate this hypothesis (Fig. 6E). The relationship of Nb/Y greater than 0.6 and the development of the negative Eu anomalies in some samples do not rule out the presence of an intraplate component in the Garamilla Formation. Because of the chemical characteristics of the volcanic rocks discussed above, it is believed that these rocks maintain a magmatic arc signature. However, their location in the eastern border of the marine Jurassic Neuquén Basin, far away from the Jurassic trench, make it difficult to reconcile the geochemical signature with the Jurassic geological scenario recognized for this area.

Therefore, these features could reveal the existence of inherited subduction components compatible with an extensional tectonic environment where the rocks were erupted.

5. Geochronology of the Garamilla Formation

In order to obtain a precise age of the Garamilla Formation, one sample of the second volcanic unit (sample Q-16) was obtained from a dacitic lapilli-tuff located at 40° 06' 35" S and 69° 48' 16" W. From that, 32 zircon grains were recovered and analyzed for geochronology at the Arizona LaserChron Center, Department of Geosciences, University of Arizona, using the procedures described by Gehrels et al. (2008).

Zircons are typically medium grained (80–200 μm diameter), and most of them

show euhedral crystal morphology, preserving faces and interfacial edges (Fig. 7A, inset). No overgrowths or metamorphic zircons with internal structures were observed. The zircons show moderate U values (109–655 ppm), and show high Th/U values consistent with a magmatic origin (>0.5). Thirty two analyses (Table 2) were conducted on single zircon crystals, among which 24 are concordant and define a weighted mean $^{206}Pb/^{238}U$ age of 187 ± 2.3 Ma (MSWD= 0.4). We interpreted this number as the timing of the magmatic crystallization of the zircons and corresponding to the deposition of the dacitic lapilli-tuff of the second eruptive unit (Fig. 7A). An average probability plot displaying the “best age” is shown in Figure 7B. Concordant late Paleozoic ages are displayed by seven grains. These and Mesoproterozoic ages registered in a single grain are considered to be xenocrysts dragged by the magmas from the country rocks during their ascent and eruption.

6. Structural analysis.

The structural analysis of the studied area was carried out using satellite imagery, mapping, profiling and the measurement of bedding, dike and fault attitudes. As showed in Figures 2 and 7C, the volcanic system is located between Cañadones Quili Mahuida and Curru Mahuida. Both Cañadones are considered here as structural lineaments and are nearly parallel with N 70–75° strikes.

These lineaments can be traced along 15 km, between the Limay River and the Campana Mahuida area, and are 7 km apart in a NNW–SSE direction.

The Quili Mahuida and Curru Mahuida lineaments are apparently truncated by N340–350° lineaments. The western border of this quasi-rectangular structure

follows the Limay River valley, which in this area has a N 330–340° strike. The above described structure strongly resembles a parallelogram with its longer axis oriented N70° (Fig. 7C). This structure can be divided into two domains: one, Quiñenao Domain, located north of the Cañadón Mencué, and the other, Fuensalida Domain, located south.

6.1. Quiñenao Domain

The Quiñenao Domain is characterized by the predominance of volcanic rocks, and the absence of sedimentary units interbedded in the volcanic sequence, making the correlation between different areas and, therefore, determining the original disposition of the volcanic beds difficult. Immediately north of Cañadón Mencué it is possible to recognize the unconformity of the surface between the volcanic and intrusive rocks. This domain is also characterized by a set of N 290–300° strike lineaments, with lengths of up to 4 km, truncated against the Curru Mahuida (ENE–WSW) and a NNW–SSE lineament. These minor lineaments are relatively straight and parallel and were assigned to fault systems. Their strikes are N 300°, which indeed is parallel to the Cañadón Mencué.

6.1. 1. Bedding attitudes

As explained above, due to the structural complexity of this domain, measurements were taken in only a few locations, where it is believed that the original position of the beds was preserved. As shown in Figure 7C, this occurs southwest and north of Puesto Quiñenao. The first locality appears alongside a prominent cliff that produces a strong topography edge. Measurement starts

immediately west of Puesto Quiñenao (Fig. 7C) and ends near Puesto Martinez. The second locality is situated 3 km northwest of Puesto Quiñenao. As displayed in Figure 7C, in the first locality bed strikes are N333°, with an average dip of 39° in a NE direction; whereas in the second locality, the average strike is N30° with dips about 16° to the SE. In the Quiñenao Domain, bedding strikes and dip directions point to a location situated immediately north of Puesto Quiñenao, making the existence of a curved structure possible. However, due to the limited quantity of data and outcrops, the northeastern and southeastern trace of this supposed structure is missing. More data are required in order to confirm the existence of such a structure.

6.1. 2. Dike attitudes

Dike attitudes (Fig. 7D) were analyzed in two localities: one in the southern margin of the Cañadón Mencué, where the dikes cut the granitic rocks with NW strikes, dipping between 54° and 65° to the southwest; the other north of the Cañadón Mencué displaying highly variable strikes, between N54°, and N300°. Considering all dikes measured in this area, the predominant (52%) eigenvector is 204°/25°. The second eigenvector (33%) is 296°/2°. The last (15%) is 30°/65°. According to these results, dikes in the Quiñenao Domain display complex arrangements, and more data are required to picture the structure.

6.1. 3. Fault attitudes

Fault attitude measurements were taken in only three localities, all near Cañadón Mencué. The first locality is situated in the lower part of the Cañadón Mencué. There, fault strikes were N52°, dipping 68° to the NW. Lineations on

fault planes indicate a dextral oblique slip fault system. The second locality is on the northern border of the Cañadón Mencué. Fault strikes are predominantly N72° dipping 63° NW. As in location 1, a dextral oblique slip fault system can be interpreted. The last locality is situated north of Cañadón Mencué, 2 km southwest of Puesto Quiñenao. There, the strike is N280°, dipping 61° NE. The lineation shows that this is a normal fault system, with the northern block moving down.

These features possibly indicate that the Quiñenao Domain was affected by tectonic subsidence, due to the existence of normal and oblique slip faults recognized in the Cañadón Mencué area.

As indicated above, numerous near parallel, longitudinal lineaments were recognized between Cañadón Mencué and the Cañadón Quili Mahuida lineament. Most of them are discontinuous, truncated by other smaller linear structures. Only three are continuous, the Cañadón Mencué, the Cañadón of Puesto Quiñenao and another located 1 km north of the Puesto. The first is more than 8 km long, but the others are between 1 and 4 km long. These small lineaments are nearly parallel and are between 700 m and 1 km apart. Our interpretation is that these lineaments represent normal faults that produce tilting of the blocks located between. These blocks display a nearly constant dip and dipping direction, about 16° to the N25–35°. The topographic difference between the upper surface of the hanging wall block and foot wall block, due to the fault movement, seems to decrease from 150 to 30 m in a NE direction, from Puesto Quiñenao to the Cañadón Quili Mahuida. Field recognition shows that the tilting and movement of the blocks seem to decrease in this direction. Because no reference levels are available, these numbers are approximate.

6.2. Fuensalida Domain

The domain located south of Cañadón Mencué is quite different. Most of it corresponds to outcrops of the Mamil Choique granite, partially covered by Quaternary sediments. Its actual upper surface dips 5 to 8° SW. The western area (Limay River) is almost completely covered by rocks of the Garamilla Formation.

6.2.1. Bedding attitudes

The volcanic rocks outcropping in the Limay River area are mostly tuff, and lapilli-tuff of rhyolitic composition. The outcrops exhibit a rounded shape about 4.5 km in diameter (Fig. 2) and their morphology is defined by a series of nearly parallel bedded tuffs and massive lapilli-tuffs (third volcanic unit). Some areas, where subvolcanic bodies are absent, display a bedded disposition (Fig. 2), useful for measuring the structural position of the volcanic levels.

The compilation of bedding values can be observed in Figure 7C in the contour diagrams (lower hemisphere). This figure shows that, in the area located immediately north and northeast of Puesto Fuensalida, the bedding dips to the northwest, with angles between 22 and 58° (Fig. 7C, E). The dip directions of the strata located 3 km north of Puesto Fuensalida points southeast with dip angles between 23 and 55° (Fig. 7F).

Finally, the bed attitudes located 3 km west of Puesto Fuensalida, on the other side of the Limay River (Neuquén province), show dip directions to the northeast, with dip values around 35°. In the last locality, the major eigenvector (66%) points 211°/52°, whereas near the Puesto Fuensalida it points 152°/48°

and that located 3 km NW points 301°/59°. These values indicate a similar dipping of these beds, with values between 30° and 45°. Dipping directions form a subcircular design pointing to a location situated a few kilometers NNW of Puesto Fuensalida, where beds show a funnel-type design (Fig. 7G).

6.2.2. Dike attitudes

Dike attitudes (Fig. 7D) were also analyzed in three localities, two of them on the western side of the Limay River and one a few kilometers east of Puesto Fuensalida. In this area, up to 86% of them strike N44°, with dips of up to 76° to the NW. In the area located 4.5 km NW of Puesto Fuensalida, they change to N350° with an average dip of 66° to the NE. The last locality, situated 6 km NW of Puesto Fuensalida, displays two populations, one up to 73% striking N36° and dipping to the SE, and the other (26%) striking N313°, dipping SW.

As indicated above, the structural disposition of the volcanic beds indicates a subcircular design with the Puesto Fuensalida area located near the center of an ellipsoidal figure. The dikes' design also presents a circumferential pattern, with its northern border following the trace of the Cañadón Quili Mahuida. The southern border of this structure follows instead the trace of the Cañadón Curru Mahuida.

6.2.3. Fault attitudes

As only a small amount of fault evidence was detected, systematic measurements of the fault attitudes were not taken.

7. Discussion and correlations

7.1. Depositional processes

Several partial profiles, examined and measured in the studied area, allow us to build a composite profile for the Garamilla Formation. It forms an 810 m thick (Fig. 8) sequence of volcanic rocks that unconformably cover the Mamil Choique Formation. Three composed volcanic units where recognized in the Puesto Quiñenao area and only two in the Puesto Fuensalida area.

The initial volcanic unit outcrops exclusively north of the Puesto Quiñenao area and extends in a NE–SW direction along 8 km. It is composed of three major interbedded lithofacies represented by lava-like ignimbrites, porphyritic massive rhyolite and microgranular massive rhyolites. It is partially cover by dacitic lapilli-tuffs belonging to the second volcanic unit.

The lava-like ignimbrite facies are uniform along their extension. These facies were possibly formed in association with the porphyritic massive rhyolite.

The lava-like ignimbrites represent intense welding pyroclastic density currents, wherein pyroclast outlines are completely obliterated and exhibit a “granophyric texture” (McArthur et al., 1998).

This microgranular fabric is interpreted by the last authors as being as a result of partial melting and recrystallization of juvenile fragments or spherulitic aggregates, which are developed where elevated temperatures and pressures are sustained over a long period of time. The vapor phase also promotes these types of textures (Lofgren, 1971). The continuity of the volcanic activity may also be responsible for the development of such features.

The classical model of ignimbrite deposition (Branney and Kokelaar, 1997, 2002) establishes the existence of rapid and sustained gradational processes

which recorded the compositional change during the eruption, evidenced by vertical compositional zoning in the ignimbrite.

However, no evidence of compositional zoning was preserved in this lithofacies.

The porphyritic massive rhyolite becomes more abundant westward of the Puesto Quiñenao area, which suggests the presence of an emission center in that direction.

In the western sector of the Puesto Quiñenao, as shown in Figure 2, the microgranular massive rhyolites appear. These lithofacies are characterized by the dominance of exsolution textures in the phenocrysts of K-feldspar. The micrographic textures are interpreted in terms of a change in the thermodynamic conditions that reach a eutectic condition where K-feldspar and quartz crystallization is coeval. The modification in magma crystallization could be explained in terms of system depressurization and/or a change in volatile contents. Therefore, the existence of a shallow high silica magmatic chamber could not be ruled out, which, together with the abundance of porphyritic lava-flows in this area, points to the existence of an eruptive vent in the proximity.

The second volcanic unit is a composed andesitic to dacitic sequence, constituted by lava-flows and welded and partially welded ignimbrite deposits (mLT), up to 20 m thick, covering the Mamil Choique Formation in the Puesto Fuensalida area.

The porphyritic massive andesite outcrops are not well preserved near Puesto Quiñenao and those observed in Puesto Fuensalida do not display lithological variations.

The pyroclastic event (massive lapilli-tuff, and eutaxitic lapilli-tuff of dacitic composition) presents inverse grading of the lithic fragments and normal

grading of juvenile fragments. These characteristics allow the consideration of the existence of a waxing period in the pyroclastic density current, generated by the presence of a highly unsteady (short lived) phenomenon.

A highly unsteady pyroclastic density current can be formed by the collapse of a lava dome or lateral decompression jets. Emplacement of lava domes and subvolcanic bodies could create the pressure increase in the magmatic chamber (Cas and Wright, 1987). The second volcanic unit concluded with the emission of dacitic lava-flows that indicate depressurization of the magmatic system.

The third volcanic unit is initiated with good-sorting, parallel bedded tuff lithofacies, with minor cross-stratification. This feature indicates a traction-dominated flow, where the finest grained clasts were transported by turbulent fluids.

Pyroclastic deposits with this characteristic are generally reported as ground-surge currents and are usually located at the base of the ignimbrite deposits. The last are represented by massive lapilli-tuffs, which are the most common ignimbrite lithofacies in the literature (Sparks, 1976; Branney and Kokelaar, 1997).

Due to the above described characteristics, it is considered that they were derived from plinian eruptive columns sustained over a considerable time. Their collapse generated low-welded ignimbrites, interpreted as a compound-cooling unit. The massive tuff-breccias are generally massive monomictic deposits that represent block-and-ash flow associated with the collapse and avalanche of lavas and/or lava domes. The block-and-ash-flow deposits are highly variable in thickness and present very low continuity along the depocenter occurring as

terraces and ledges.

The intensity of the volcanic activity increases progressively with the deposition of massive lithic breccias. This lithofacies outcrops in the Cañadón Mencué area and is interpreted as a coarse and proximal facies of ignimbrite deposits generated by the collapse of plinian columns.

The small rounded bodies, 20 to 50 m in diameter, formed by vertical flow banded rhyolites, are interpreted as representing the coherent lava-dome facies, whereas the elongated-narrow levels were interpreted as rhyolite lava-flows. The lava-domes and lava-flows that are related to the massive tuff-breccia lithofacies possibly represent the end of the volcanic activity.

The last igneous activity was recorded by rhyolitic dikes that exhibit a circumferential pattern in the Limay River area and a more complex pattern in the Puesto Quiñenao area.

7.2. Geochronology of the Garamilla Formation and its relationship with equivalent units of the Neuquén Basin

In order to establish the correlation between the analyzed unit and those equivalents of the Neuquén Basin, we compare radiometric dating, as well as the geological characteristics shared by the units. In the southern sector of the Neuquén Basin, in the Piedra del Aguila area, located 10 km west of the studied area, Ferello (1947) described the Piedra del Aguila Formation, assigning an Early Jurassic age due to the existence of Liassic flora. The unit was considered to represent the “Precuyano Cycle” of Gulisano et al. (1984). The age was subsequently confirmed by Spalletti et al. (2010) using U-Pb dating in zircon (191.7 ± 2.8 Ma). This unit is covered by the Sañicó Formation, which

consists of andesitic lava-flows, dacitic tuffs and, according to Galli (1969), rests over the Piedra del Aguila Formation.

D'Elia et al. (2012a) describe three sections in the Sañicó Formation, starting with lava-flows of andesitic composition. The middle section is composed of pyroclastic rocks of rhyolitic to rhyodacitic compositions. It concludes with an upper section comprising andesitic lava-flows and epiclastic sedimentary rocks with interbedded limestones. As indicated above, the volcanic succession of the Garamilla Formation can be compared with those of the Sañicó Formation. The age established for the Garamilla Formation in the Quiñenao area is 187 ± 2.3 Ma (U-Pb, zircon), making a straight correlation between both units possible.

Bermúdez et al. (2002) reported a significant sequence 2,500 m thick in the subsurface of the central area of the Neuquén Basin. The rocks belong to the Cerro Bandera depocenter, along the western sector of the Dorsal de Huincul. This depocenter is located 150 km northward (Fig.1) and the sequence starts with a lower section formed by phenoandesitic lava-flows intercalated with sedimentary rocks. The middle section is characterized by an intercalation of sedimentary rocks (siltstones and sandy siltstones) with tuffs and pyroclastic flows, whereas the upper section is composed of phenorhyolitic crystalloclastic tuffs. The age is considered to be between 216 and 244 Ma (Pángaro et al., 2002) and therefore to represent an extensional stage (Precuyano Cycle) previous to the development of the marine basin.

Schiuma and Llambías (2008) and Llambías et al. (2007) studied a volcanic sequence in the Anticlinal Campamento depocenter, also located in the western portion of the Dorsal de Huincul. They described lava-flows and block-and-ash deposits of andesitic, dacitic and rhyolitic compositions, as well as, ignimbrites

and fall-deposits rich in silica. These rocks were assigned to the Late Triassic (Rhaetian)-Early Jurassic (Hettangian) time from U-Pb isotope studies in igneous zircons (199.0 ± 1.5 Ma andesite lava-flow and 203.75 ± 0.26 Ma dacite breccia).

The so called Precuyano Cycle (Gulisano et al., 1984) represents the first stage of extension, prior to the marine transgression in the Neuquén Basin. The above cited units share many stratigraphic and chemical similarities and represent an extensional stage that can be recognized along the central and southern part of the basin. This period of extension starts in the Triassic and can be traced into the Middle Jurassic. Therefore, the Lower Jurassic volcanism recognized in the central portion of the Neuquén Basin, as well as in its southeastern border, in the Piedra del Aguila area, can be continued into the western portion of the Nordpatagonian Massif, making a direct correlation between the volcanism of the Garamilla Formation and those of the Neuquén Basin, such as the Sañicó, Lapa, Sierra de Chacaico and equivalent formations.

7.3 Geochemistry and tectonic settings of equivalent units of the Neuquén Basin and the Nordpatagonian Massif.

As indicated above, Bermúdez et al. (2002) described rocks that can be related with the Precuyano Cycle of the Neuquén Basin (Gulisano et al., 1984). According the geochemical data (Bermúdez et al., 2002) these rocks display chemical composition between those of andesite and rhyolite, belonging to a subalkaline series. The trace and rare earth elements were plotted against normalized values of chondrite and N-MORB and the results are shown in Figure 9A and B. Figure 9A displays an envelope of the igneous rocks

considered to belong to the Precuyano Cycle, including those of Bermúdez et al. (2002). Compared with out samples from the Garamilla Formation, the concentration of LILE is similar, including the negative anomaly of Nb. A different behavior is related to the positive anomaly of Pb in our samples, which indicates a major contribution of sedimentary material during subduction. According to Schiuma and Llambías (2008) the Precuyano volcanic rocks drilled in the Norte de la Dorsal and Anticlinal Campamento areas are andesite and dacite in composition. Figure 9B shows their results plotted together with other Precuyano volcanic rocks, contrasted with chondrite in an extended normalized diagram. The design displays characteristics of subduction-related rocks, such as the highly positive anomalies of LILE, negative Ta and Nb and highly negatives Sr, P and Ti.

D'Elia et al. (2012b) analyzed the geochemical characteristics of several Precuyano volcanic units, including those outcropping in the Cordillera del Viento, Chachil, Dorsal de Huincul and Piedra del Aguila areas. Their results were plotted with our samples of the Garamilla Formation in Figure 9C and D. Figure 9C indicates that most rocks were plotted in the volcanic arc field in the Y versus Nb diagram of Pearce et al. (1984). A portion of the population of the Marifil Group samples (Pankhurst and Rapela, 1995) plot in the intraplate field, possibly due to the minor influence of subduction components during their evolution. Figure 9D displays the REE normalized to chondrite diagram. As observed in the above cited figures, samples of the Garamilla Formation follow the trend marked by other Precuyano volcanic rocks. Our samples are located in an intermediate position between the Precuyano samples of D'Elia et al. (2012b) and those of the Marifil Complex. This behavior can be related to the

position of the Garamilla samples, which are located east of those of D'Elia et al. (2012b) and west of those of the Marifil Complex.

As indicated by D'Elia et al. (2012b), rocks from the Cordillera del Viento, Chachil, Dorsal de Huincul and Piedra del Aguila areas mostly belong to the calc-alkaline series with trace element patterns typical of the orogenic series. However, the sequence shows some evolutionary and compositional differences (> 50% differentiated acidic terms) compared with the classic arc series. Also, its similarity with the rocks of the Marifil Complex allows for the suspicion of some differences compared with the classical subduction-related volcanic arcs. Therefore, our interpretation favors an intraplate setting of emplacement for the volcanic rocks of the Garamilla Formation related to extensional conditions.

7.4 Structural characteristics of the Quiñenao-Fuensalida area and comparison with structures of a similar age

The compilation of the attitudes of bedding in Figure 7C show that the dip directions of the strata in the Fuensalida area converge toward a position located a few kilometers north of Puesto Fuensalida. The dip angles of the bedding also increase toward this position. Dikes are usually considered as a result of near-field or local stress. The incomplete development of a circumferential dikes pattern in this area could be related to an incomplete formation of a ring-fault system.

Two possibilities were invoked by Acocella and Neri (2009) in order to explain the local stress in the volcanic structure. One is considering the existence of a pressurized shallow magma reservoir, and the other is the load of a volcanic

edifice. No evidences of a shallow magmatic reservoir or related rocks were detected during field recognition, but the second possibility cannot be excluded. As displayed in Figure 2, the outcrops in the Fuensalida area show an ellipsoidal shape, consistent with the attitude of the volcanic bedding and dike disposition. Therefore, the existence of a volcanic edifice in the Fuensalida area cannot be ruled out. In the Quiñenao area, dikes also point to a curved structure, but the data is insufficient to clearly define the design, although, a few kilometers west, the outcrops of the microgranular massive rhyolite point to the existence of a shallow magmatic acidic reservoir associated with the volcanic system.

As indicated by Figures 2 and 7, the volcanic system in the Fuensalida-Quiñenao area is located in a near parallelogram structure. Its northern and southern borders are N 70–75° fault systems called, respectively, the Quili Mahuida and Curru Mahuida lineaments. A major, curvilinear N290–300° structure (the Cañadón Mencué) represents a hinge zone that divides the Quiñenao-Fuensalida structure. North of the hinge zone several N290–300° normal and oblique slip faults produce NE tilting of the blocks, which point to a NE–SW extension (N30°–50°). The extensional regime and the fault-driven subsidence north of the hinge zone produced enough room to accommodate the volcanic sequences recognized in the Quiñenao area.

A trapdoor structure could be indicated for the area located south of the hinge zone (Cole et al., 2005), facilitated by the existence of an incomplete ring-fault system. The result could due to asymmetrical block subsidence (Fig. 9E).

Our preliminary interpretation of the Quili Mahuida and Curru Mahuida lineaments is that the deformation was produced by a dextral transtensional

system developed on Upper Paleozoic rocks. This deformational event can be assigned to a regional stress field also recognized in the southern part of the Neuquén Basin. There, several NE–SW Precuyano depocenters are subparallel to the Limay River (Sañicó, Piedra del Aguila, China Muerta, El Sauce, Loma Pedregosa, Borde del Limay, and Rio Limay, Vergani et al., 1995), and were produced by extensional faults during the Late Triassic-Early Jurassic episode of rifting. The volcanic system recognized in both areas north and south of the hinge zone, was deposited in the open spaces generated during fault movement.

This structure strongly remembers those half-grabens located in the eastern part of the Neuquén Basin (Vergani et al., 1995; Franzese and Spalletti, 2001; Franzese et al., 2006; Cristallini et al., 2009).Accordingly, the area located north of the hinge zone can be considered as a half-graben depocenter, similar to those of the Neuquén Basin and named here as the Quiñenao depocenter.

In contrast, south of the hinge zone the deformation is dominated by a near local stress, possibly generated by the weight of the volcanic edifice, while regional deformation is masked by this local stress field.

The Quili Mahuida and Curru Mahuida lineaments have a similar trend that others recognized in the western Nordpatagonian Massif. The Patú Co and El Loro lineaments (Bjerg et al., 1997), located east of El Cuy, display a similar design with strikes between N60° and N85°. These lineaments also affected Upper Paleozoic granitic rocks.

The trends of the Quili Mahuida and Curru Mahuida lineaments are also similar to those of the “A” lineament described by Gregori et al. (2008), which extends between Salitral Bajo de Menucos and Chimpay. These lineaments are

believed to be related to the Gondwanide Orogeny of northern Patagonia (Gregori et al., 2008), but more information is required in order to constrain the time and cinematic of the deformational event recorded in the Quiñenao-Fuensalida area.

8 Conclusions

The facial, stratigraphic, petrographic and geochemical analyses of the volcanic rocks of the Garamilla Formation in the Puestos Fuensalida and Quiñenao areas reveal a complex volcanic sequence formed by three volcanic units. The geochemical studies have shown an evolution from normal calc-alkaline to high-K calc-alkaline series, the preponderance of the peraluminous rocks over metaluminous, and an increase in high-field element negative anomalies along the volcanic activity development.

These elements point to a progressive change from an initial subduction-related volcanism to one of intraplate-related volcanism.

Radiometric U-Pb dating has demonstrated that the Garamilla Formation in the Fuensalida and Quiñenao area is of Early Jurassic age. This volcanic activity is temporally and geochemically equivalent to similar volcanic units located in half-grabens in several areas of the Neuquén Basin and the eastern area of the Nordpatagonian Massif. The Fuensalida and Quiñenao areas show two different structural designs divided by a hinge zone. The northern zone was interpreted as a transtensional half-graben, whereas the southern exhibits a trapdoor structure. The trends of lineaments that bound the volcanic system in the Fuensalida-Quiñenao area (Quili Mahuida and Curru Mahuida lineaments) were also recognized in western Nordpatagonian Massif, which were assigned to the

Gondwanide Orogeny.

Acknowledgements

This study is part of the PhD of Leonardo Benedini, granted by research projects“Configuración Gondwánica del sector occidental de la Comarca Nordpatagónica, Argentina”, Pict BID 2007 N° 01649, FONCYT, and “Configuración geológica y geodinámica del sector central de la Comarca Nordpatagónica, Argentina (24/H100), Universidad Nacional del Sur.

We would like to thank José Kostadinoff and Gastón Alvarez, for help during field trips and fructiferous discussions about the geophysical and geological configuration of the western Nordpatagonian Massif. Many thanks to the Fuensalida, Quiñenao, Jaramillo, Arias, and Cortes families, that allowed us access to their lands, gave us shelter and helped throughout the many field trips.

Constructive and thoughtful reviews by two anonymous colleagues and Dr. Victor Ramos on the early version greatly improved the same and they are truly thanked.

References

Acocella, V., Neri, M., 2009. Dike propagation in volcanic edifices: Overview and possible developments. Tectonophysics, 471, 67–77.

Benedini, L., Gregori, D. A., 2012.La Formación Garamilla: evento volcánico del Jurásico Inferior del sector occidental de la Comarca Nordpatagónica, Provincia

de Río Negro, Argentina. Aportes al Magmatismo y Metalogénesis. Serie Correlación Geológica, 28, 9–26. San Miguel de Tucumán.

Bermúdez, A., Delpino, D., Pángaro, F., 2002. Volcanismo de arco asociado a procesos de subducción - extensión durante el Triásico Superior - Jurásico Inferior (Precuyano). Área Cerro Bandera, Cuenca Neuquina, Argentina.4 Congreso de Exploración y Desarrollo en Hidrocarburos, Actas en CD. Mar del Plata.

Bjerg, E.A., Gregori, D.A., Labudía, C.H., 1997, Geología de la región de El Cuy, Macizo de Somoncura, provincia de Río Negro. Asociación Geológica Argentina, Revista, 52, 3, 387–399.

Branney, M.J., Kokelaar, B.P., 1997. Giant bed from a sustained catastrophic density current flowing over topography: Acatlan ignimbrite, Mexico. Geology, 25, 115–118.

Branney, M.J., Kokelaar, P., 2002. Pyroclastic density currents and the sedimentation of ignimbrites. Geological Society, London, Memoir, 27, 143 pp.

Cas, R.A.F., Wright, J.W., 1987. Volcanic successions: Modern and ancient. Chapman & Hall.London, 528 pp.

Cerredo, M., López de Luchi, M., Ostera, H., Cagnoni, M., Linares, E., 2000.Amphibolic tonalites in the south western North Patagonian

Massif.Geochemistry, Age and Tectonic Setting.9 Congreso Geológico Chileno, Puerto Varas, Actas 2: 712–715.

Cingolani, C., Dalla Salda, L., Hervé, F., Munizaga, F., Pankhurst, R.J., Parada, M.A., Rapela, C.W., 1991.The magmatic evolution of northern Patagonia; New impressions of pre-Andean tectonics. Geological Society of America Special Paper,265, 29–43 pp.

Coira, B., 1979. Descripción Geológica de la Hoja 40d, Ingeniero Jacobacci, Provincia del Río Negro. Boletín 168. Servicio Geológico Nacional, 101 pp. Buenos Aires.

Cole, J.W., Milner, D.M., Spinks, K.D., 2005. Calderas and caldera structures: a review. Earth-Science Reviews 69, 1–26.

Cristallini, E., Tomezzoli, R., Pando, G., Gazzera, C., Martínez, J.M., Quiroga, J., Buhler, M., Bechis, F., Barredo, S., Zambrano, O., 2009.Controles precuyanos en la estructura de la Cuenca Neuquina. Asociación Geológica Argentina, Revista, 65, 2, 248–264.

Cucchi, R., Espejo, P., González, R., 1998. Geología y recursos naturales de la Hoja 4169-I Piedra del Águila, Río Negro y Neuquén. Subsecretaría de Minería de la Nación, SEGEMAR, Buenos Aires, Boletín 242, 74 pp.

Dalla Salda, L.H., Varela, R., Cingolani, C.A., Aragón, E. 1994.The Rio Chico

Paleozoic crystalline complex and the evolution of Northern Patagonia. Journal of South American Earth Sciences, 7, 1–10.

D'Elia, L., Muravchik, M., Franzese, J.R., López, L., 2012a.Tectonostratigraphic analysis of the Late Triassic–Early Jurassic syn-rift sequence of the Neuquén Basin in the Sañicó depocentre, Neuquén Province, Argentina. Andean Geology, 39, 1, 133–157.

D'Elia, L., Muravchik, M., Franzese, J.R., Bilmes, A., 2012b. Volcanismo de sin-rift de la Cuenca Neuquina, Argentina: relación con la evolución Triásico Tardía-Jurásico Temprano del margen andino. Andean Geology, 39, 1, 106–132.

Féraud, G., Alric, B., Fornari, M., Bertrand, H., Haller, M., 1999.^{40}Ar/^{39}Ar dating of the Jurassic volcanic province of Patagonia: migrating magmatism related to Gondwana break-up and subduction. Earth and Planetary Science Letter, 172 83–96.

Ferello, R., 1947. Los depósitos plantíferos de Piedra del Águila (Neuquén) y sus relaciones. Boletín de Informaciones Petroleras, 278, 248–261. Buenos Aires.

Franzese, J.R., Pankhurst, R.J., Rapela, C.W., Spalletti, L.A., Fanning, M.,

Muravchik, M., 2002.Nuevas evidencias geocronológicas sobre el magmatismo Gondwánico en el noroeste del Macizo Nordpatagónico. 15 Congreso Geológico Argentino, Actas en CD, El Calafate.

Franzese, J.R., Spalletti, L.A., 2001. Late Triassic–Early Jurassic continental extension in southwestern Gondwana: tectonic segmentation and pre-break-up rifting. Journal of South American Earth Sciences, 14, 257–270.

Franzese, J.R., Veiga, G.D., Schwarz, E., Gómez-Pérez, L., 2006. Tectono-stratigraphic evolution of a Mesozoic graben border system: the Chachil depocentre, southern Neuquén Basin, Argentina. Journal of the Geological Society of London, 163, 207–221.

Galli, C.A., 1969. Descripción geológica de la Hoja 38c Piedra del Águila, provincias de Neuquén y Río Negro. Servicio Nacional Minería y Geología Boletín 111, 67 pp. Buenos Aires.

Gehrels, G.E., Valencia, V.A., Ruiz, J., 2008. Enhanced precision, accuracy, efficiency, and spatial resolution of U-Pb ages by laser ablation–multicollector–inductively coupled plasma–mass spectrometry: Geochemistry, Geophysics Geosystems, Q03017, doi: 10.1029/2007GC001805.

Gill, J., 1981.Orogenic andesites and plate tectonics.Springer-Verlag, Berlín, 390 pp.

Gregori, D.A., Kostadinoff, J., Strazzere, L. Raniolo, A., 2008. Tectonic significance and consequences of the Gondwanide orogeny in northern Patagonia, Argentina. Gondwana Research, 14, 429–450.

Gulisano, C.A., Gutiérrez Pleimling, A.R., Digregorio, R.E., 1984. Esquema estratigráfico de la secuencia jurásica del oeste de la Provincia de Neuquén. 9 Congreso Geológico Argentino, Bariloche, Actas 1, 236–259.

Gust, D., Biddle, K., Phelps, D., Uliana, M., 1985.Associated middle to late Jurassic volcanism and extension in southern South America. Tectonophysics, 116, 223–253.

Hervé, F., Calderón, M., Fáundez, V., 2008.The metamorphic complexes of the Patagonian and Fuegian Andes.Geologica Acta, 6, 1, 43–53.

Homovc, J., Constantini, L., Pellon de Miranda, A., Ferreira, R., 1996. Evolution of the Deseado Massif in Argentina, and its relationship with the San Julian offshore area in the South Atlantic Ocean. YPF S.A. Argentina, Petrobras Internacional Brazil.

Kostadinoff, J., Gregori, D., Raniolo, A., 2005. Configuración Geológica Geofísica del sector norte de la Provincia de Río Negro. Revista de la Asociación Geológica Argentina. 60, 368-376.

Le Bas, M.J., Le Maitre, R.W., Streckeisen, A., Zanettin, B., 1986. A chemical

classification of volcanic rocks based on the total alkali-silica diagram. Journal of Petrology, 27, 745–750.

Linares, E., Cagnoni, M.C., Do Campo, M., Ostera, H.A., 1988. Geochronology of metamorphic and eruptive rocks of southeastern Neuquén and northwestern Río Negro Provinces, Argentine Republic. Journal of South American Earth Sciences, 1, 53–61.

Llambías, E.J., Leanza, H.A., Carbone, O., 2007. Evolución tectono-magmática durante el Pérmico al Jurásico Temprano en la Cordillera del Viento (37°05´S – 37°15´S): nuevas evidencias geológicas y geoquímicas del inicio de la cuenca Neuquina. Asociación Geológica Argentina, Revista, 62, 217–235.

Lofgren, G., 1971. Experimentally produced devitrification textures in natural rhyolite glass. Geological Society of America, 82, 111–124.

López de Luchi, M.G., Ostera, H.A., Cerredo, M.E., Linares, E., Haller, M.J., Cagnoni, M.C., 1999.Unravelling the ages of the crystalline basement at Sierra de Mamil Choique, Río Negro, Argentina.2 Simposio de Geología Isotópica, Villa Carlos Paz, Anales 34, SEGEMAR, Buenos Aires, 322–326.

López de Luchi, M.G., Ostera, H.A., Cerredo, M.E., Cagnoni, M.C., Linares, E., 2000.Permian magmatism in Sierra de Mamil Choique, North Patagonian Massif, Argentina.9 Congreso Geológico Chileno, Puerto Varas, Chile, Actas 2, 750-754.

McArthur, A.M., Cas, R.A.F., Orton, G.J., 1998. Distribution and significance of crystalline, perlitic and vesicular textures in the Ordovician Garth Tuff (Wales).Bulletin of Volcanology. 60, 260–285.

McPhie, J., Doyle, M., Allen, R., 1993. Volcanic textures: a guide to the interpretation of textures in volcanic rocks. Tasmanian Government Printing Office, Tasmania, 198 pp.

Mpodozis, C., Ramos, V.A., 2008. Tectónica Jurásica en Argentina y Chile: extensión, subducción oblicua, rifting, deriva y colisiones. Revista de la Asociación Geológica Argentina, 63, 4, 481–497.

Nullo, F.E., 1978. Descripción geológica de la Hoja 41dc, Lipetrén.Provincia de Río Negro.Boletín 158. Servicio Geológico Nacional,Buenos Aires, 88 pp.

Nullo, F.E., 1979. Descripción geológica de la Hoja 39c, Paso Flores. Provincias de Río Negro y Neuquén. Boletín 167. Servicio Geológico Nacional,Buenos Aires, 70 pp.

Núñez, E., Cucchi, R.J., 1990. Estratigrafía del sector noroccidental del Macizo Nordpatagónico en los alrededores de Mencué, provincia del Río Negro, República Argentina. 11 Congreso Geológico Argentino, San Juan, Actas 2: 125–128.

Núñez, E., Cucchi, R.J., 1997. Geología y petrografía de Trapalcó, Provincia del Río Negro. Asociación Geológica Argentina, Revista, 52, 297–310.

Orchuela, I.A., Ploszkiewicz, J.V., 1984. La Cuenca Neuquina. In: Ramos, V.A.; (editor). Relatorio de la Geología y recursos naturales de la Provincia de Río Negro. 9 Congreso Geológico Argentino, 163–188 pp.

Pángaro, F., Corbera, R., Carbone, O., Hinterwimmer, G. 2002. Los reservorios del Precuyano. In: Schiuma, M., Hinterwimmer, G.; Vergani G. D.; (editors) Rocas Reservorio de las Cuencas Productivas Argentinas. Instituto Argentino del Petróleo y del Gas, Buenos Aires, 229–254 pp.

Pankhurst, R.J., Rapela, C.W., Caminos, R., Llambías, E., Párica, C.A., 1992.Revised age of the central Somuncura batholith, North Patagonian Massif. Journal of South American Earth Sciences, 5, 321–325.

Pankhurst, R.J., Rapela, C.W., 1995, Production of Jurassic rhyolite by anatexis of the lower crust of Patagonia. Earth and Planetary Science Letters, 134, 23–36.

Pankhurst, R.J., Rapela, C.W., Fanning, C.M., Márquez, M., 2006.Gondwanide continental collision and the origin of Patagonia. Earth Science Reviews, 76, 3–4, 235–257.

Pearce, J.A., 1982. Trace element characteristics of lavas from destructive plate

boundaries. In: Thorpe, R.S. (editor). Andesites: Orogenic Andesites and related rocks. Wiley & Sons, New York, 525–554.

Pearce, J.A., Harris, N.B.W., Tindle, A.G., 1984.Trace element discrimination diagrams for the tectonic interpretation of granitic rocks. Journal of Petrology, 25, 956–983.

Peccerillo, A., Taylor. S.R., 1976.Geochemistry of Eocene calc-alkaline volcanic rocks from the Kastamonu area, northern Turkey. Contribution to Mineralogy and Petrology, 58, 63–81.

Rapela, C.W., Pankhurst, R.J., 1992. The granites of northern Patagonia and the Gastre fault systems in relation to the break-up of Gondwana. In: Storey, B.C., Alabaster, T, Pankhurst, R.J., (eds) Magmatism and the causes of continental break-up. Geological Society of London, Special Publication, 68, 209–220.

Rapela, C.W., Pankhurst, R.J., Fanning, C.M., Hervé, F., 2005. Pacific subduction coeval with the Karoo mantle plume: the early Jurassic Subcordilleran belt of northwestern Patagonia. In: Vaughan, A.P.M., Leat, P.T., Pankhurst, R.J., (eds) Terrane Processes at the Margins of Gondwana, Geological Society of London Special Publications 246, 217–239.

Ravazolli, I., Sesana, F.L., 1977. Descripción geológica de la Hoja 41c, Río Chico, Provincia de Río Negro. Boletín 148. Servicio Geológico Nacional, 78

pp. Buenos Aires.

Schiuma, M., Llambías, E.J., 2008. New ages and chemical analysis on Lower Jurassic volcanism close to the Huincul High, Neuquén. Asociación Geológica Argentina, Revista, 63, 4, 644–652.

Sesana, F., 1968.Rasgos petrológicos de la comarca de Río Chico, Río Negro. Terceras Jornadas Geológicas Argentinas, Actas 3, 99–107.

Shand, S.J., 1951. Eruptive rocks.Their genesis, composition, classification, and their relation to ore-deposits, Fourth Edition. Wiley and Sons, New York, 488 pp.

Spalletti, L.A., Franzese, J.R., Morel, E., D'Elia, L., Zúñiga, A., Fanning, C.M., 2010. Consideraciones acerca de la sedimentología, paleobotánica y geocronología de la Formación Piedra del Águila (Jurásico Inferior, Neuquén, República Argentina). Asociación Geológica Argentina, Revista, 66, 3, 305–313.

Sparks,S.J., 1976.Grain size variations in ignimbrites and implications for the transport of pyroclastic flows. Sedimentology, 23,147–188.

Sun, S.S., McDonough, W.F., 1989. Chemical and isotopic systematics of oceanic basalts: implication for mantle composition and processes. In: Saunders, A.D., Norry, M.J., (eds), Magmatism in the Ocean basins, Geological

Society Special Publication, 42, 313–345.

Thompson, R.N., 1982. British tertiary volcanic province. Scottish Geology 18, 49–107.

Vergani, G.D., Tankard, A.J., Belotti, H.J., Welsink, H.J., 1995. Tectonic evolution and paleogeography of the Neuquén Basin, Argentina. In: Tankard, A.J., Suárez Soruco, R., Welsink, H.J., (editors) Petroleum Basins of South America. American Association of Petroleum Geologists, Memoirs, 62, 383–402.

Volkheimer, W., 1964. Estratigrafía de la zona extrandinas del Departamento de Cushamen (Chubut) entre los paralelos 42° y 42°30´ y los meridianos 70° y 71°. Asociación Geológica Argentina, Revista, 19, 85–107.

Winchester, J.A., Floyd, P.A., 1977.Geochemical discrimination of different magma series and their differentiation products using immobile elements. Chemical Geology, 20, 325–343.

FIGURE CAPTIONS

Figure 1: Geological sketch of northern Patagonia showing the distribution of principal outcrops of the Jurassic volcaniclastic units, as well as the Jurassic-Cretaceous Colorado and Neuquén Basins that border the Nordpatagonian Massif. The Huincul (according to Orchuela et al, 1984, Kostadinoff et al., 2005 and Gregori et al., 2008) and Gastre fault zones, also considered as boundaries

of the Nordpatagonian Massif, are shown. The older volcaniclastic units are the Triassic Los Menucos Formation and Late Triassic-Early Jurassic Precuyano deposits. Jurassic magmatism is represented by the Marifil, Garamilla and Taquetrén Formation. The Jurassic Subcordilleran Batholith, located west of the Nordpatagonian Massif includes arc-related intrusive rocks. Location of Figure 2 is also displayed.

Figure 2: Geological map of the Quiñenao-Fuensalida area. The distribution of the three volcanic units of Garamilla Formation is shown. The studied area is located between the Cañadones Quili Mahuida and Currú Mahuida. In the central part, a Quaternary cover precludes establishing the architecture of the volcanic rocks.

Figure 3: A) Columnar joints in lava-like ignimbrites north of Puesto Quiñenao. Hammer in the lower margin of the picture as scale. B) “Granophyric texture” (McArthur et al., 1998) in lava-like ignimbrites showing equigranular, anhedral crystals of quartz and K-feldspar. C) Typical outcrop of porphyritic massive rhyolite located 1 km west of Puesto Martinez. D) Porphyritic texture showing euhedral K-feldspar, plagioclase and quartz phenocrysts in a sericitic altered fine-grained groundmass. E) Microgranular massive rhyolite outcrop located 2 km west of Puesto Martinez. Most borders of this body seems to by nearly vertical. F) Micrographic texture in euhedral to subhedral quartz and K-feldspar crystals.

Figure 4: A) Outcrop near Puesto Fuensalida showing the porphyritic massive

dacite of the second volcanic unit covered by massive lapilli-tuffs of the third unit. B) Euhedral to subhedral phenocrysts of zoned plagioclase embedded in a fine-grained groundmass. C) Massive lapilli-tuffs of dacitic composition showing eutaxitic texture. Outcrop located southwest of Puesto Quiñenao. D) Lithic fragment of migmatite embedded in a glassy groundmass. E) Typical outcrops of the third volcanic units west of Puesto Quiñenao. Massive lapilli-tuff displaying a lobular morphology is partially cover by massive tuff-breccia and porphyritic massive and flow banding rhyolites.

Figure 5: A) Typical outcrop of parallel bedded tuff near Puesto Quiñenao, located in the base of a pyroclastic succession of the third volcanic unit. B) Microphotograph of aligned crystal of quartz K-feldspar in a glassy groundmass. C) Ignimbritic lobe 30 m thick 2 km north of Puesto Fuensalida. D) Small lithic and juvenile fragments softy deformed in a fine-grained groundmass 2 km north of Puesto Fuensalida. E) Representative outcrop of the Massive tuff-breccias displaying a chaotic texture composed of angular fragments of rhyolitic lava-flow. Hammer as a scale. F) Massive lithic breccia outcropping 1 km northeast of Puesto Martinez showing large fragments of massive lapilli-tuffs and granitic rocks. G) Nearly vertical flow banding in a subrounded rhyolitic body, north of Puesto Fuensalida.

Figure 6: A) Peccerillo and Taylor's (1976) diagram displaying a normal to a high-K calc-alkaline trend typical of continental magmatic arcs with a predominance of acidic composition. B) Le Bas et al.'s (1986) diagram showing rhyolitic to andesitic composition for the volcanic sequence. C) Shand's (1951)

diagram displaying a metaluminous character for the second volcanic unit and dominantly peraluminous for the other two. D) Winchester and Floyd's (1977) SiO_2 vs. Zr/TiO_2 diagram indicates that most samples are of rhyolitic and dacitic composition. E) Normalized to chondrite (Thompson, 1982) expanded diagram displaying negative anomalies of Nb and Ta, indicative of subduction-related fluids during evolution of the volcanic rocks. F) Chondrite normalized REE diagram (Sun and McDonough, 1989) of samples of Garamilla Formation, showing small negative Eu anomalies indicative of plagioclase fractionation. Flat HREE illustrate that garnet was not involved during melting of the parental magma. G) Rb vs Y + Nb diagram (Pearce et al., 1984) indicating that all samples plot in the field of magmatic arc-related rocks. H) The same result was obtained in the Nb vs Y diagram (Pearce et al., 1984).

Figure 7: A) Cathodoluminescence image of typical zircons of the Garamilla Formation. They are medium grained (80–200 μm diameter), with a euhedral morphology preserving faces and interfacial edges. Concordant ages are displayed by 24 grains. A weighted mean $^{206}Pb/^{238}U$ age of 187 ± 2.3 Ma was obtained. B) Probabilistic plot of $^{206}Pb/^{238}U$ ages displaying the "best age" for Garamilla Formation. C) Satellite imagery of the studied area displaying bedding attitude results. D) Satellite imagery of the studied area displaying dike attitude results. E) This picture shows the area located north of Puesto Fuensalida where a sequence of parallel bedded tuffs and massive lapilli-tuffs are dipping NW. F) Outcrops located 3 km north of Puesto Fuensalida displaying same lithofacies as E) dipping SE. G) Funnel-type design in massive lapilli-tuff a few kilometers NNW of Puesto Fuensalida.

Figure 8: Composite profile for the Garamilla Formation as documented by several minor profiles measured in the Fuensalida-Quiñenao area. The first volcanic unit, mainly outcropping in the Quiñenao area is composed of acidic facies. The second unit includes intermediate to mild acidic pyroclastic and lava-flow facies, with minor thickness. The last is 400 m thick and is represented by an acidic composition that includes tuffs, lapillis, breccias and lava-flows.

Figure 9: A) Normalized to NMORB (Sun and McDonough, 1989) diagram of the Precuyano Cycle volcanic rocks, compared with Garamilla Formation samples. All display a significant negative Nb anomaly. Garamilla Formation samples show a positive Pb anomaly. B) Chondrite normalized expanded diagram (Sun and McDonough, 1989) of Precuyano deposits which are strongly similar to samples of Garamilla Formation. C) Y vs. Nb diagram (Pearce et al., 1984) showing that all samples from Precuyano deposits and Garamilla Formation plot in the volcanic arc granite field. Several samples of Marifil Formation plot in the within-plate field of granitic rocks. D) Normalized to chondrite REE diagram shows a very similar design for Precuyano deposits of the Neuquén basin, and the Marifil and Garamilla formations of the Nordpatagonian Massif. E) Geological cross section for the Fuensalida-Quiñenao area during eruption of the Garamilla Formation. The half-graben domain of the Quiñenao area is separated from the trapdoor domain of the Fuensalida area by the “hinge” zone along the Cañadón Mencué

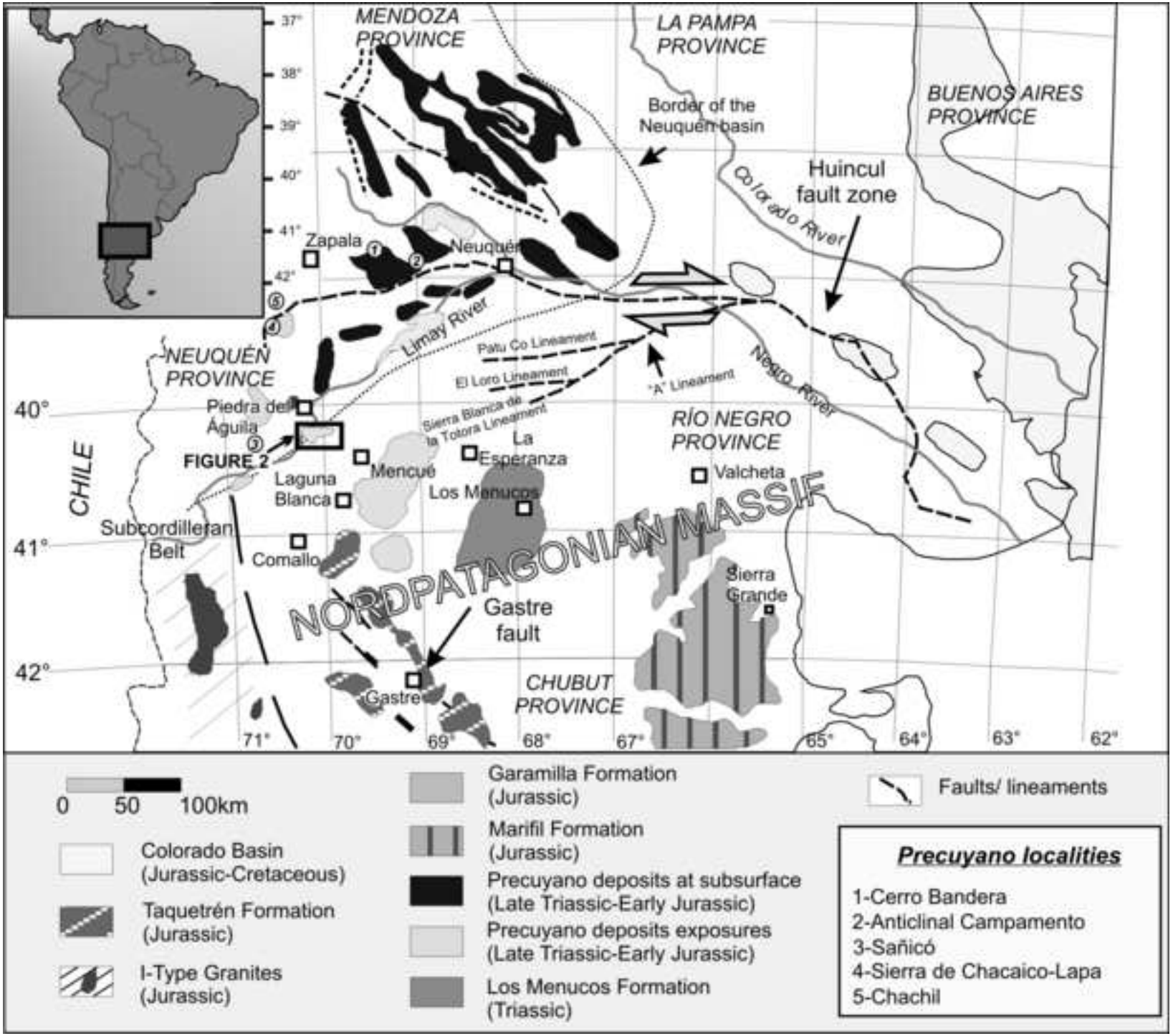
MENDOZA PROVINCE
LA PAMPA PROVINCE
BUENOS AIRES PROVINCE
Border of the Neuquén basin
Huincul fault zone
Colorado River
Zapala
Neuquén
Limay River
Patu Co Lineament
El Loro Lineament
Sierra Blanca de la Totora Lineament
"A" Lineament
Negro River
NEUQUÉN PROVINCE
RÍO NEGRO PROVINCE
Piedra del Águila
FIGURE 2
Laguna Blanca
Mencué
La Esperanza
Valcheta
Los Menucos
CHILE
Subcordillerian Belt
Comallo
NORDPATAGONIAN MASSIF
Sierra Grande
Gastre fault
Gastre
CHUBUT PROVINCE
37°
38°
39°
40°
41°
42°
71°
70°
69°
68°
67°
65°
64°
63°
62°
0 50 100km
Colorado Basin (Jurassic-Cretaceous)
Taquetrén Formation (Jurassic)
I-Type Granites (Jurassic)
Garamilla Formation (Jurassic)
Marifil Formation (Jurassic)
Precuyano deposits at subsurface (Late Triassic-Early Jurassic)
Precuyano deposits exposures (Late Triassic-Early Jurassic)
Los Menucos Formation (Triassic)
Faults/ lineaments
Precuyano localities
1-Cerro Bandera
2-Anticlinal Campamento
3-Sañicó
4-Sierra de Chacaico-Lapa
5-Chachil

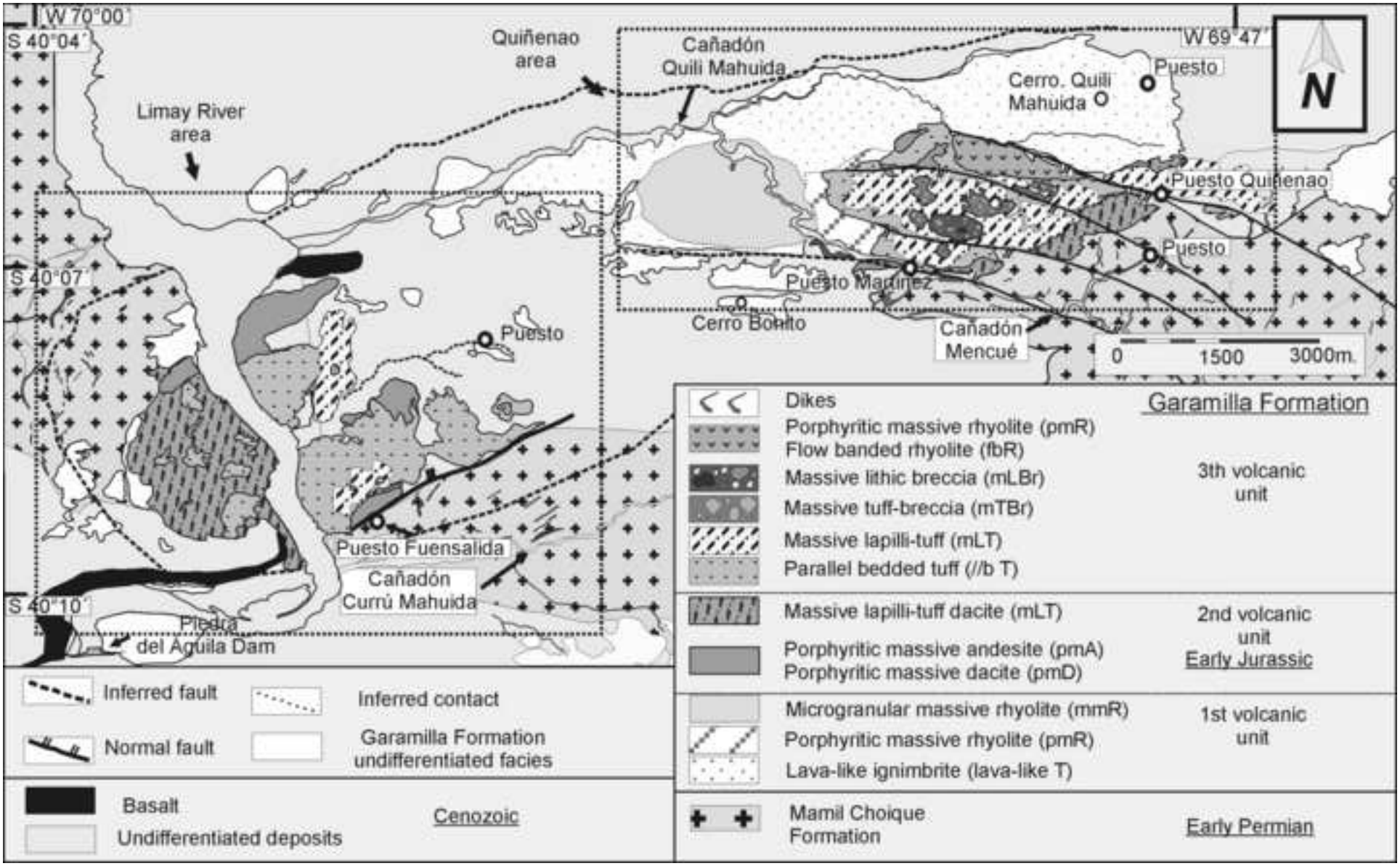
W 70°00'
S 40°04'
S 40°07'
S 40°10'
W 69°47'
N
Quiñenao area
Cañadón Quili Mahuida
Limay River area
Cerro. Quili Mahuida
Puesto
Puesto Quiñenao
Puesto
Puesto Martínez
Cerro Bonito
Cañadón Mencué
Puesto
0
1500
3000m
Puesto Fuensalida
Cañadón Currú Mahuida
Piedra del Aguila Dam
Dikes
Porphyritic massive rhyolite (pmR)
Flow banded rhyolite (fbR)
Massive lithic breccia (mLBr)
Massive tuff-breccia (mTBr)
Massive lapilli-tuff (mLT)
Parallel bedded tuff (//b T)
Garamilla Formation
3th volcanic unit
Massive lapilli-tuff dacite (mLT)
Porphyritic massive andesite (pmA)
Porphyritic massive dacite (pmD)
2nd volcanic unit
Early Jurassic
Micrograniular massive rhyolite (mmR)
Porphyritic massive rhyolite (pmR)
Lava-like ignimbrite (lava-like T)
1st volcanic unit
Mamil Choique Formation
Early Permian
Inferred fault
Normal fault
Inferred contact
Garamilla Formation undifferentiated facies
Basalt
Undifferentiated deposits
Cenozoic

Figure 3

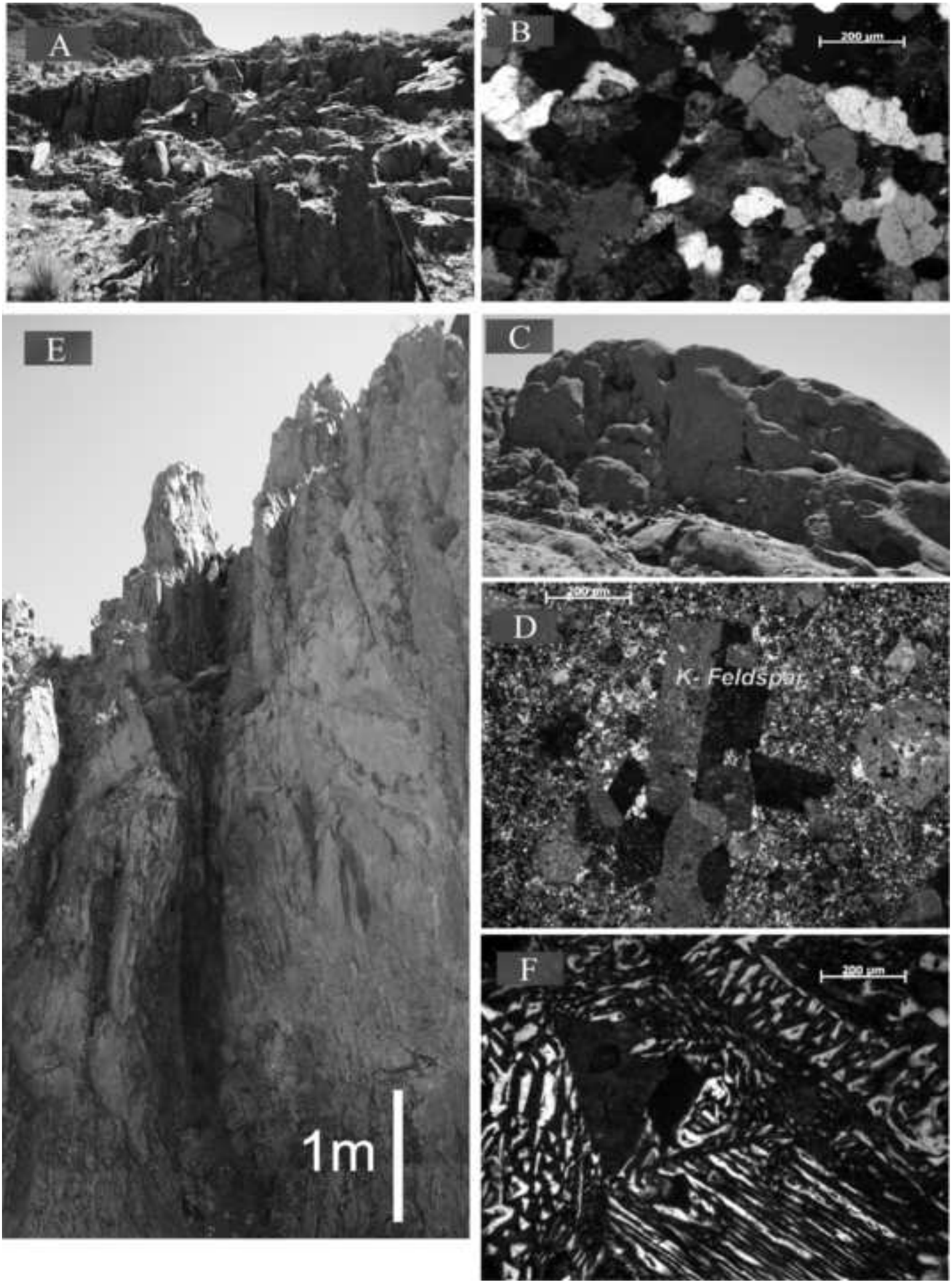

Figure 4

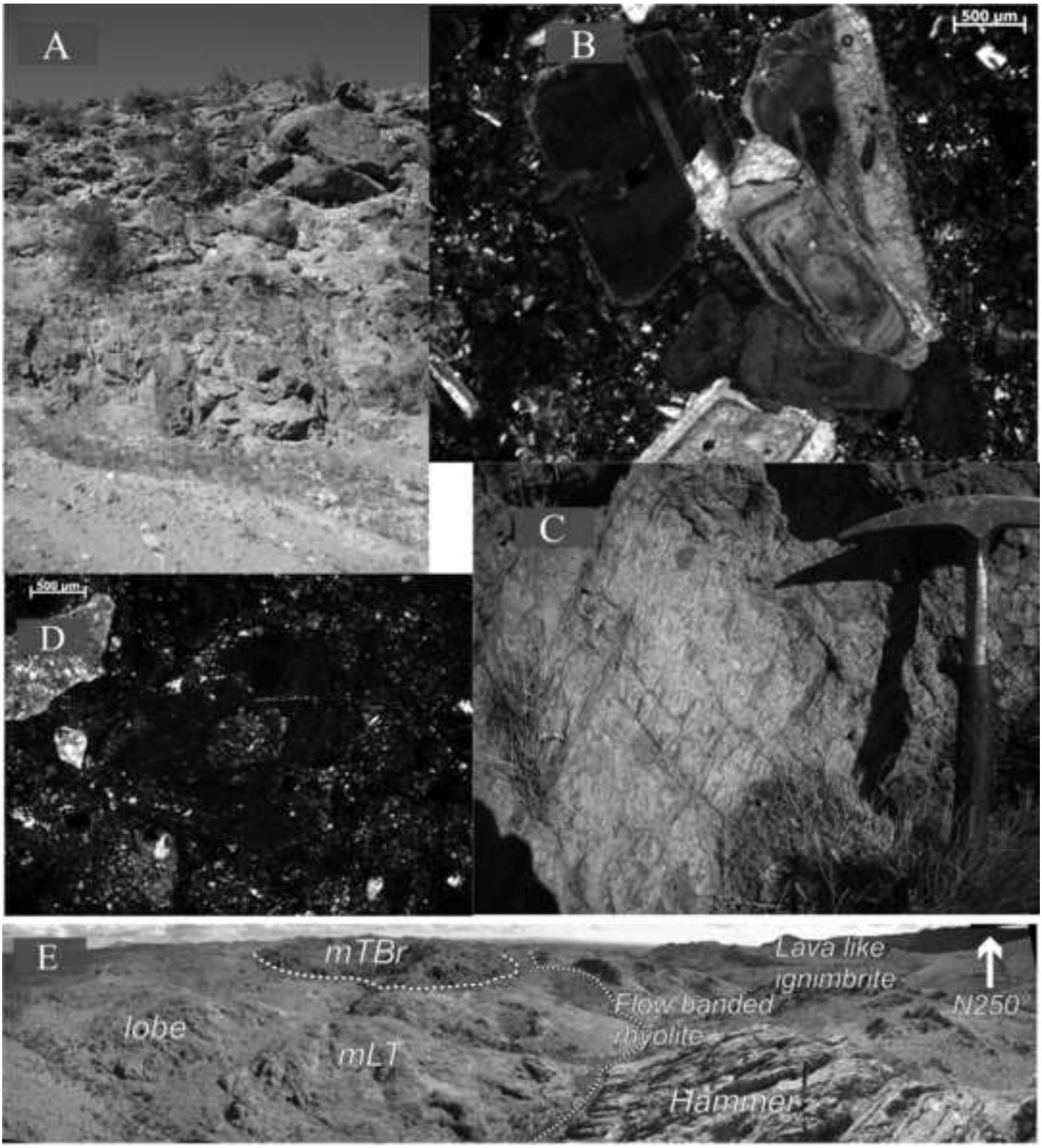

Figure 5

Figure 6

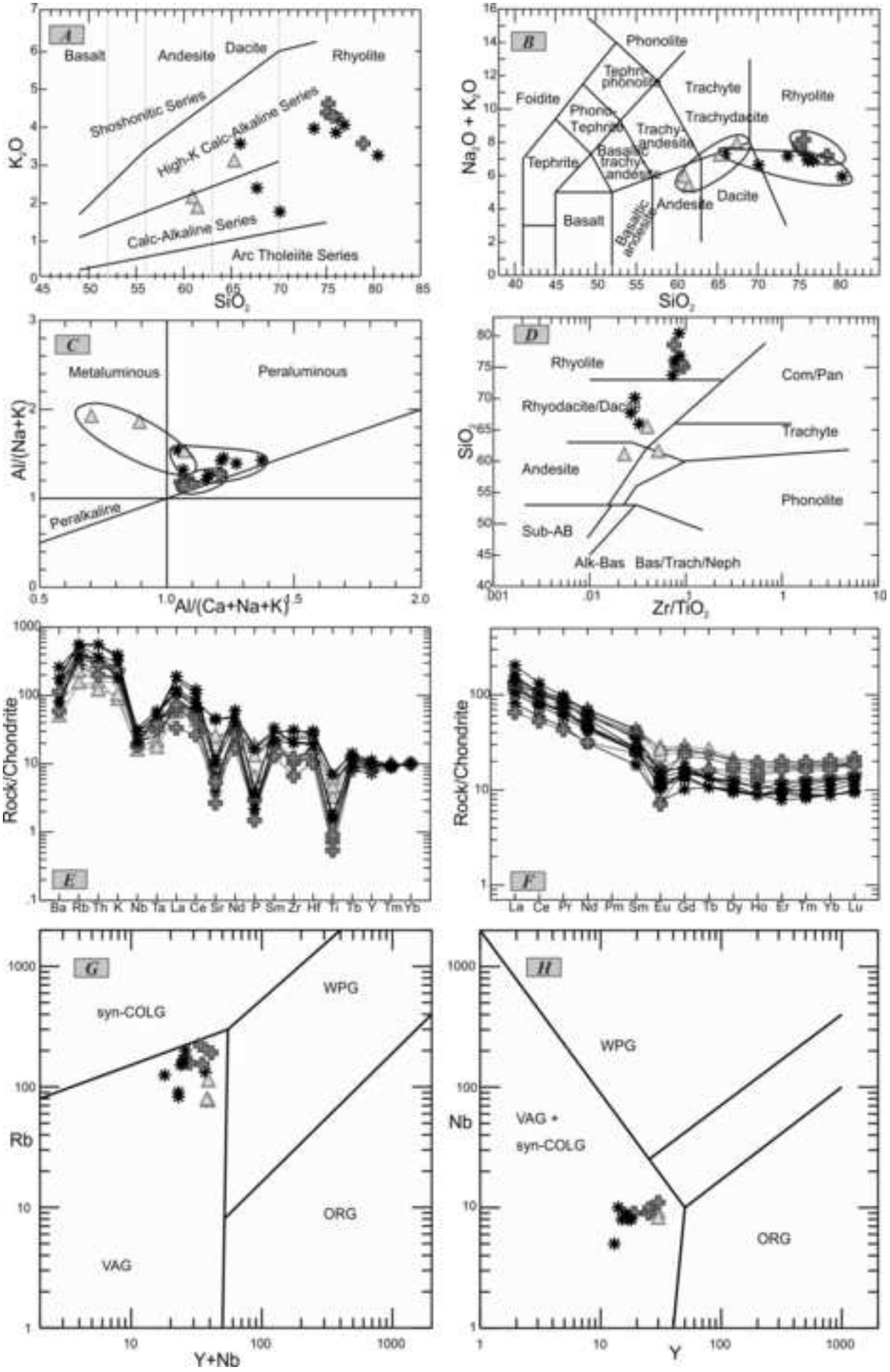

Figure 7

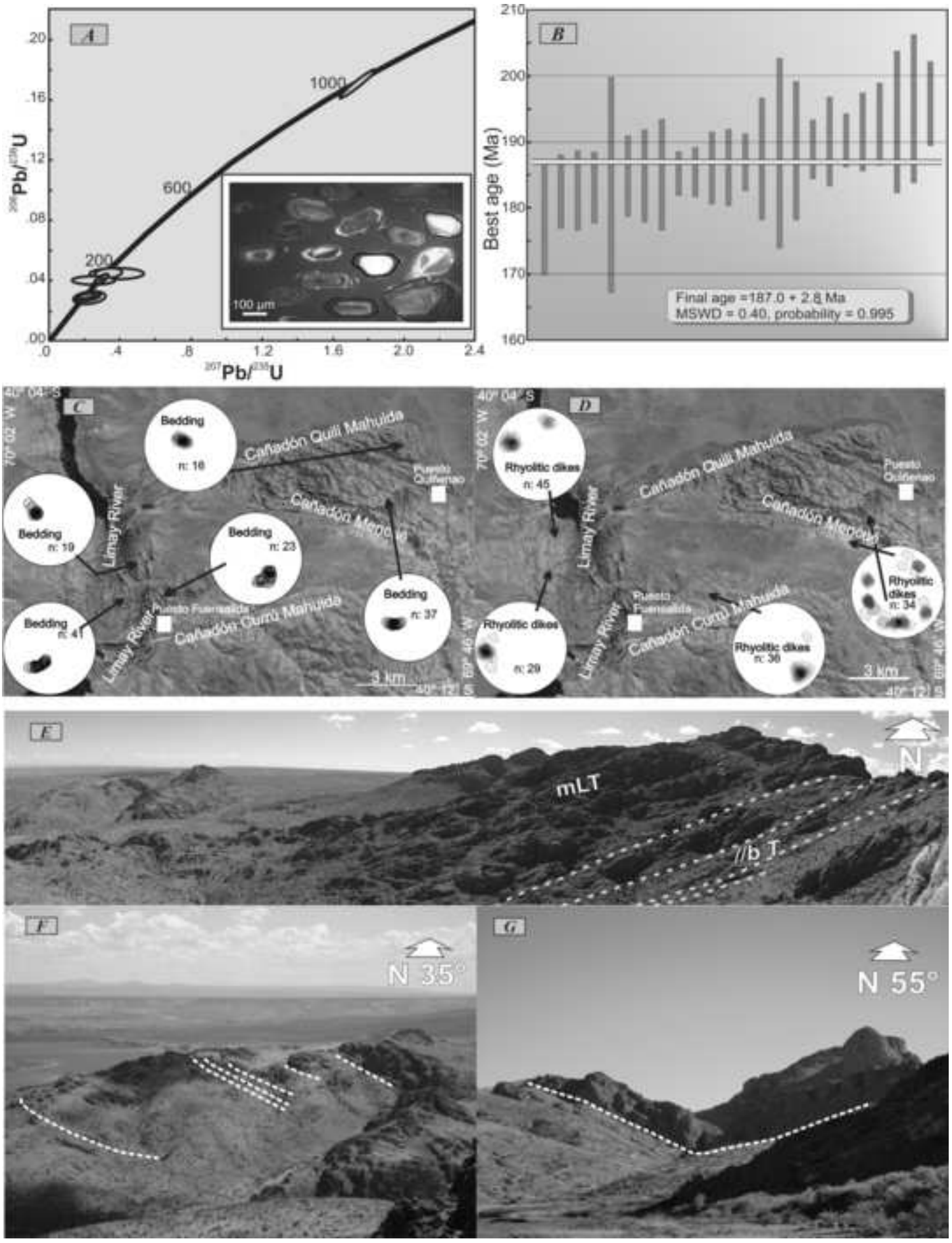

Figure 8

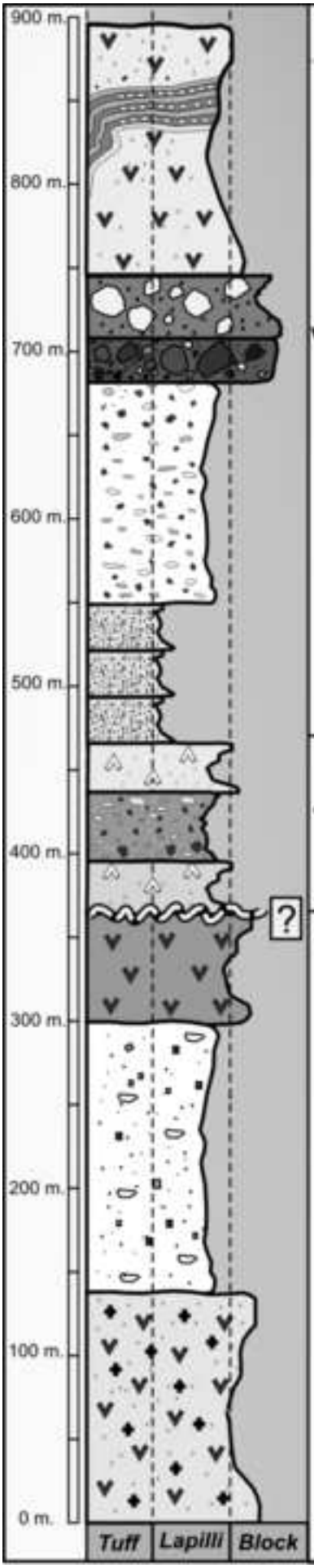

	Facies description	Interpretation
THIRD VOLCANIC UNIT	Porphyritic massive rhyolite (pmR) and flow banded rhyolite (fbR)	Lava flow, lava dome and syn-volcanic intrusion coherent facies
	Massive tuff-breccia (mTBr)	Block and ash flow deposits, dome collapse avalanche
	Massive lithic-breccia (mLBr)	Unsteady pyroclastic density current (Waxing phase)
	Massive lapilli-tuff (mLT) non-graded	
	Parallel bedded tuff (//b T)	Turbulent dilute current (pyroclastic surge deposits)
SECOND VOLCANIC UNIT	Porphyritic massive dacite (pmD)	Lava flow or lava dome coherent facies
	Massive lapilli-tuff (mLT) inversely graded Lithic and normal graded juvenile	Waning pyroclastic density current
	Porphyritic massive andesite (pmA)	Lava flow coherent facies
FIRST VOLCANIC UNIT	Porphyritic massive rhyolite (pmR) tabular development	Lava flow, lava dome or syn-volcanic intrusion coherent facies
	Lava-like ignimbrite (Lava-Like T): columnar jointing, uniform, stratified "granophyric texture"	Sustained pyroclastic density current deposits
	Microgranular massive rhyolite (mmR): micrographic texture, rounded and massive	Shallow magma reservoir

Figure 9

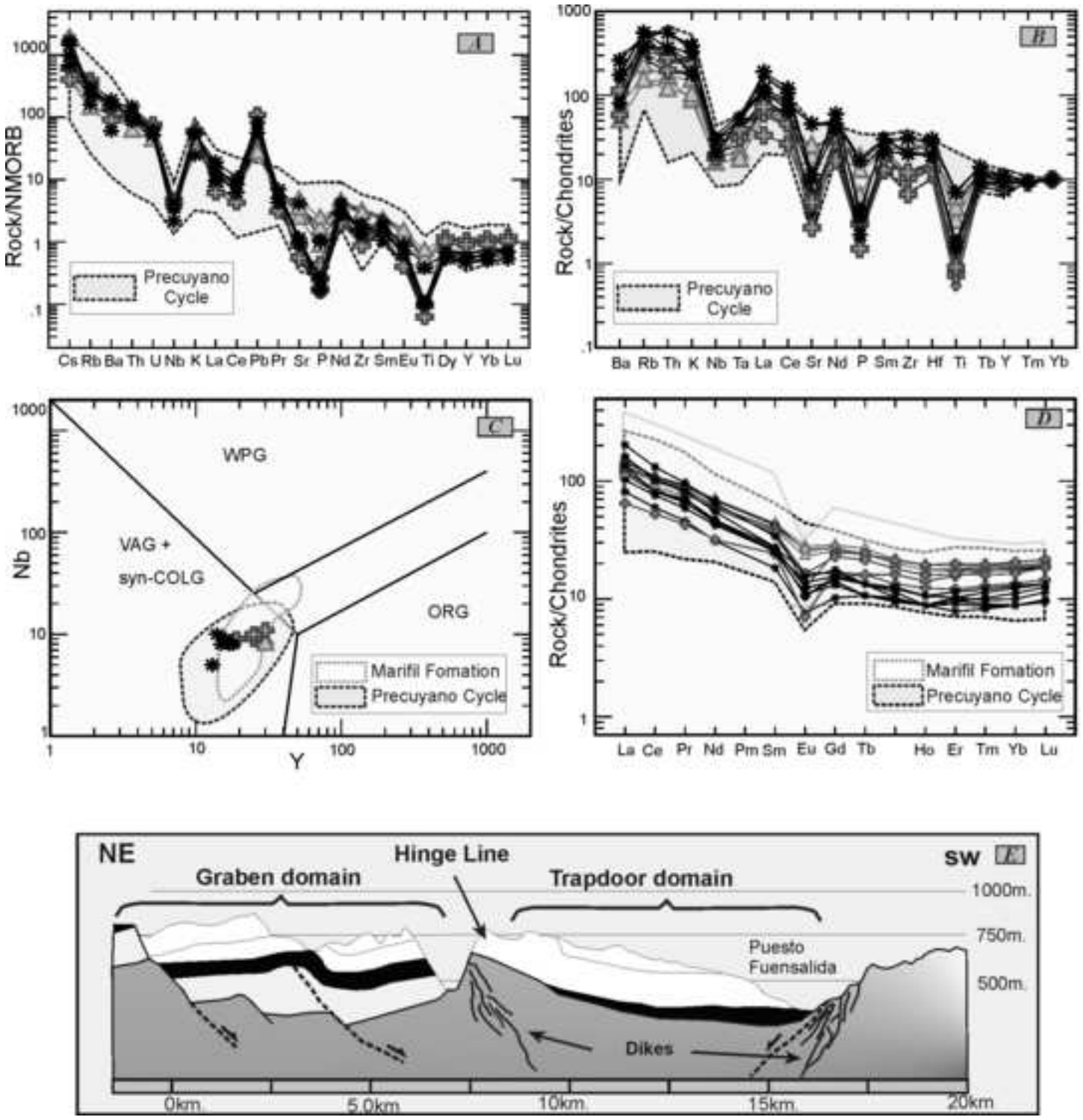

Table 1: Chemical composition of the analyzed samples. (All samples were collected in the area of Puesto Quiñenao)

Sample	Q6	Q7	Q12	Q16	Q20	Q22	Q24	Q25	Q26	Q27	Q8	Q4	Q2	Q19	Q21
volcanic unit	2	1	3	2	3	2	2	2	1	1	1	3	3	3	3
SiO_2	67.7	78.57	76.19	61.46	80.43	65.95	65.32	60.95	75.22	75.08	75.71	73.71	76.03	76.88	70.11
Al_2O_3	15.44	11.55	12.45	14.77	11.35	15.4	15.37	15.75	12.65	12.44	12.62	13.91	11.69	11.44	14.07
FeO	5.06	1.42	1.38	5.05	1.17	4.82	5.03	7.60	1.48	1.92	2.16	2.01	1.78	1.40	4.55
Fe_2O_3(T)	4.55	1.28	1.24	4.54	1.05	4.34	4.53	6.84	1.33	1.73	1.94	1.81	1.60	1.26	4.09
MnO	0.05	0.02	0.05	0.16	0.02	0.10	0.09	0.09	0.06	0.06	0.04	0.06	0.02	0.02	0.02
MgO	0.50	0.10	0.11	0.97	0.10	1.37	1.61	2.33	0.14	0.15	0.16	0.19	0.14	0.10	0.59
CaO	1.55	0.35	0.46	7.31	0.18	2.63	2.34	5.02	0.29	0.69	0.47	1.00	0.26	0.43	0.94
Na_2O	5.53	3.70	2.64	3.45	2.68	3.72	4.10	3.77	3.01	3.52	3.87	3.20	3.32	2.83	4.84
K_2O	2.40	3.50	4.25	1.88	3.26	3.57	3.10	2.14	4.62	4.38	4.29	3.97	3.86	4.06	1.78
TiO_2	0.51	0.11	0.08	0.49	0.10	0.68	0.66	0.92	0.08	0.12	0.12	0.14	0.13	0.14	0.49
P_2O_5	0.13	0.02	0.02	0.10	0.02	0.20	0.19	0.28	0.03	0.05	0.02	0.03	0.03	0.02	0.12
LOI	1.31	0.25	1.33	4.04	1.00	2.18	1.48	1.21	0.81	0.91	0.89	1.51	1.49	1.31	1.62
Total	99.68	99.45	98.82	99.18	100.20	100.10	98.79	99.29	98.23	99.14	100.10	99.53	98.57	98.50	98.68
Sc	10.00	3.00	2.00	10.00	3.00	12.00	12.00	19.00	3.00	4.00	3.00	3.00	3.00	2.00	10.00
V	50	7	4	52	4	70	83	144	6	3	5	14	10	6	74
Ba	709	745	1190	515	947	959	1042	824	572	892	1000	963	1222	1046	381
Sr	355	55	47	215	73	350	305	429	79	50	81	104	87	101	368
Y	15	19	18	30	14	27	30	30	25	30	25	17	13	16	15
Zr	137	81	67	254	81	224	262	211	64	112	106	103	96	120	145
Cr	10	10	10	10	10	10	10	10	10	10	19	18	17	19	20
Co	7	1	1	1	1	6	9	12	1	1	1	1	1	1	5
Ni	18	18	18	18	18	18	18	18	18	18	17	20	17	18	17
Ga	14	13	13	27	13	18	17	19	14	15	17	21	10	12	14
Rb	83	158	200	75	152	132	110	77	222	192	154	157	125	168	90
Nb	8	9	8	9	10	10	9	8	9	11	10	8	5	9	8
Cs	11.70	2.90	6.00	2.80	3.70	12.30	2.80	13.30	6.70	4.20	2.80	12.10	9.90	4.80	6.80

La	27.10	27.60	28.50	36.70	19.30	34.50	31.20	26.90	15.40	31.90	30.60	48.20	38.40	32.00	24.30
Ce	50.00	52.20	51.80	66.80	36.40	66.60	60.60	53.70	32.20	63.70	64.00	80.60	62.40	49.50	46.50
Pr	6.24	6.29	6.27	8.86	4.37	8.56	7.91	7.23	4.08	8.11	7.55	9.20	7.84	6.71	5.61
Nd	21.80	20.90	20.80	32.80	14.50	32.00	29.00	28.40	14.80	28.60	27.20	30.20	25.70	22.00	19.80
Sm	4.20	4.00	4.00	6.70	2.80	6.50	5.90	6.10	3.70	6.00	5.60	5.20	4.20	3.80	3.90
Eu	0.96	0.62	0.61	1.62	0.44	1.49	1.33	1.52	0.41	0.73	0.95	0.89	0.72	0.64	0.80
Gd	3.40	3.20	3.10	5.90	2.10	5.60	5.30	5.60	3.50	5.10	4.70	3.60	2.90	2.70	3.20
Tb	0.50	0.60	0.50	1.00	0.40	0.90	0.90	0.90	0.60	0.90	0.80	0.50	0.40	0.40	0.50
Dy	2.90	3.40	3.20	5.50	2.50	5.10	5.10	5.40	4.10	5.40	4.60	3.10	2.40	2.60	2.60
Ho	0.50	0.70	0.60	1.10	0.50	1.00	1.00	1.10	0.80	1.10	0.90	0.60	0.50	0.50	0.50
Er	1.60	2.00	1.90	3.20	1.70	2.90	3.00	3.20	2.60	3.30	2.70	1.70	1.30	1.60	1.50
Tm	0.23	0.33	0.31	0.50	0.29	0.45	0.47	0.49	0.44	0.50	0.41	0.25	0.21	0.26	0.22
Yb	1.50	2.30	2.20	3.30	2.10	3.00	3.10	3.20	3.10	3.50	2.80	1.70	1.50	1.90	1.50
Lu	0.25	0.37	0.34	0.51	0.34	0.47	0.49	0.49	0.49	0.55	0.47	0.29	0.24	0.32	0.25
Hf	4.10	3.00	2.60	7.10	3.00	6.40	7.00	5.90	2.90	4.20	3.80	3.10	2.70	3.30	3.70
Ta	0.80	0.80	0.80	0.70	0.80	0.70	0.60	0.50	1.30	1.00	1.00	0.80	0.70	0.90	0.80
Pb	19.00	33.00	14.00	25.00	14.00	15.00	14.00	8.00	25.00	23.00	20.00	25.00	23.00	17.00	25.00
Th	10.60	11.00	10.20	9.90	11.60	10.80	9.90	7.20	16.80	13.30	15.00	17.90	15.80	13.30	10.50
U	2.70	2.80	2.10	2.50	3.10	2.80	2.60	2.00	3.60	3.20	3.00	2.40	2.50	2.80	3.00

Analyst: ACTLABS

Table 2: U-Pb geochronological analyzes.

Sample Q16		Isotope ratios									Apparent ages (Ma)							
Analysis	U (ppm)	206Pb/ 204Pb	U/Th	206Pb*/ 207Pb*	± (%)	207Pb* /235U*	± (%)	206Pb* /238U	± (%)	Error corr	206Pb* /238U*	± (Ma)	207Pb* /235U	± (Ma)	206Pb*/ 207Pb*	± (Ma)	Best age (Ma)	± (Ma)
Q16 - 27R	246	22270	1.7	20.7803	11.1	0.1864	12.1	0.0281	4.9	0.40	178.6	8.5	173.5	19.3	105.3	262.5	178.6	8.5
Q16 - 26R	239	21176	2.8	21.2097	9.9	0.1867	10.4	0.0287	3.0	0.29	182.5	5.5	173.8	16.5	56.7	236.7	182.5	5.5
Q16 - 18R	655	25050	3.1	20.8056	4.7	0.1905	5.7	0.0287	3.2	0.57	182.7	5.8	177.0	9.3	102.4	111.0	182.7	5.8
Q16 - 21R	579	29289	2.9	19.8101	5.1	0.2005	5.9	0.0288	2.9	0.49	183.1	5.2	185.6	10.0	217.1	118.6	183.1	5.2
Q16 - 20	109	5464	1.3	17.2249	24.8	0.2312	26.4	0.0289	8.9	0.34	183.5	16.2	211.2	50.3	531.9	551.0	183.5	16.2
Q16 - 7R	409	46166	2.7	20.5807	9.9	0.1948	10.4	0.0291	3.3	0.31	184.8	6.0	180.8	17.3	128.1	233.7	184.8	6.0
Q16 - 3R	506	28733	3.7	19.9360	5.9	0.2012	7.0	0.0291	3.8	0.54	184.8	6.9	186.1	12.0	202.4	137.5	184.8	6.9
Q16 - 22C	487	13930	1.6	19.4779	5.2	0.2061	6.9	0.0291	4.5	0.65	185.0	8.2	190.3	12.0	256.1	120.4	185.0	8.2
Q16 - 9R	439	31772	2.8	20.2320	7.8	0.1987	8.0	0.0292	1.7	0.22	185.2	3.2	184.0	13.4	168.1	181.6	185.2	3.2
Q16 - 19R	601	25234	2.1	19.9751	2.8	0.2014	3.4	0.0292	2.0	0.58	185.4	3.6	186.3	5.8	197.9	64.9	185.4	3.6
Q16 - 14R	319	7115	2.4	20.1669	11.2	0.2003	11.6	0.0293	2.9	0.25	186.1	5.3	185.3	19.6	175.6	261.6	186.1	5.3
Q16 - 1R	276	12207	3.4	19.5216	9.3	0.2069	9.8	0.0293	3.1	0.31	186.1	5.6	191.0	17.1	251.0	215.0	186.1	5.6
Q16 - 16R	495	15785	2.4	18.3763	9.0	0.2208	9.3	0.0294	2.3	0.25	187.0	4.2	202.6	17.0	388.4	201.9	187.0	4.2
Q16 - 13R	345	13187	2.3	20.2678	8.9	0.2007	10.2	0.0295	4.9	0.48	187.4	9.0	185.7	17.2	164.0	208.5	187.4	9.0
Q16 - 9C	386	3126	2.7	17.8425	15.9	0.2290	17.7	0.0296	7.6	0.43	188.3	14.2	209.4	33.5	454.2	355.7	188.3	14.2
Q16 - 15C	200	2738	1.8	17.6857	12.3	0.2316	13.5	0.0297	5.6	0.41	188.7	10.3	211.5	25.7	473.7	272.1	188.7	10.3
Q16 - 17C	579	12910	4.1	18.3363	10.9	0.2236	11.2	0.0297	2.3	0.21	188.9	4.3	204.9	20.7	393.3	245.9	188.9	4.3
Q16 - 24R	452	14277	3.1	20.9433	5.1	0.1970	6.2	0.0299	3.5	0.57	190.1	6.6	182.6	10.4	86.8	121.0	190.1	6.6
Q16 - 10R	384	5206	1.5	19.7811	9.7	0.2088	9.9	0.0300	2.1	0.21	190.2	3.9	192.5	17.3	220.5	223.8	190.2	3.9
Q16 - 22R	264	9448	2.3	21.3072	13.3	0.1951	13.7	0.0302	3.0	0.22	191.5	5.7	181.0	22.7	45.8	319.7	191.5	5.7
Q16 - 30	395	17919	1.5	21.1989	10.5	0.1973	10.9	0.0303	3.2	0.29	192.7	6.1	182.9	18.3	57.9	250.1	192.7	6.1
Q16 - 12R	232	11000	2.7	18.9086	13.7	0.2216	14.8	0.0304	5.6	0.38	193.0	10.6	203.3	27.2	323.9	311.5	193.0	10.6
Q16 - 4R	612	45876	2.0	20.2899	3.8	0.2086	6.9	0.0307	5.8	0.84	194.9	11.1	192.4	12.1	161.4	88.6	194.9	11.1
Q16 - 25C	629	5569	3.6	20.4463	6.0	0.2080	6.8	0.0308	3.2	0.47	195.8	6.2	191.8	11.8	143.4	140.0	195.8	6.2